Liikennevirasto
Finnish Transport Agency

29 • 2011
RESEARCH REPORTS OF THE
FINNISH TRANSPORT AGENCY

VILLE LEHTONEN

Instrumentation and analysis of a railway embankment failure experiment

A GENERAL SUMMARY

Ville Lehtonen

Instrumentation and analysis of a railway embankment failure experiment

A general summary

Research reports of the Finnish Transport Agency
29/2011

Finnish Transport Agency
Helsinki 2011

Photograph on the cover: Ville Lehtonen

Online publication pdf (www.liikennevirasto.fi)
ISSN-L 1798-6656
ISSN 1798-6664
ISBN 978-952-255-685-1

Finnish Transport Agency
P.O. Box 33
FIN-00521 HELSINKI, Finland
Tel. +358 20 637 373

Ville Lehtonen: Instrumentation and analysis of a railway embankment failure experiment – a general summary. Finnish Transport Agency, Construction Management. Helsinki 2011. Research reports of the Finnish Transport Agency 29/2011. 57 pages. ISSN-L 1798-6656, ISSN 1798-6664, ISBN 978-952-255-685-1.

Keywords: railway embankment, failure test, stability, instrumentation, monitoring, pore pressure

Summary

In October of 2009 Tampere University of Technology (TUT) and the Finnish Rail Administration (now part of Finnish Transport Agency) conducted a full-scale railway embankment failure experiment in Salo, Finland. Goals of the test were to collect extensive monitoring data for further development of different stability calculation methods and to test the technical suitability of different methods for monitoring the stability of embankments.

A new, small railway embankment was built in place of an old, de-commissioned blind track on a clayey soil. Four steel frameworks, each 12 meters long, were used to simulate short railway cars with bogie carriages. The frameworks were loaded with modified shipping containers which were gradually filled with sand.

The test area was extensively instrumented with 40 pore pressure gauges, 9 inclinometer tubes, 2 total stations monitoring a total of 27 prisms, 9 earth pressure gauges, 3 settlement tubes and 76 slip surface measuring pipes. In addition, the weight of the containers was measured with strain gauges on the frameworks. Acceleration gauges were used to measure the tilt angle of the containers.

The loading of the containers took place during two days. During the initial loading the displacements and pore pressures increased fairly linearly. The rates of displacement and pore pressure increase began to accelerate exponentially at about 2.5 hours before collapse, during the final stages of loading. The final train load was 87 kPa, which is equivalent to a 218 kN/m line load.

The resulting landslip (about 50 m wide along the embankment) had a distinctively wedge-shaped cross-section. A clearly defined slip surface could not be measured. Instead, the measurements point to a thicker slip zone. The entire clay mass was significantly disturbed, which would indicate a zone failure.

The amount of yield-induced excess pore pressure in the clay was significant. The time-dependency of the pore pressure and deformation response was also very apparent, as the excess pore pressure and displacements increased at an accelerating rate prior to failure, at a steady external load.

The best indicators for an impending embankment failure seem to have been settlement under the embankment and lateral displacements in the soil. For monitoring, these should be supplemented with pore pressure measurements.

Ville Lehtonen: Ratapenkereen sorrutuskokeen instrumentointi ja analysointi – yhteenvetoraportti. Liikennevirasto, rakennuttamisosasto. Helsinki 2011. Liikenneviraston tutkimuksia ja selvityksiä 29/2011. 57 sivua. ISSN-L 1798-6656, ISSN 1798-6664, ISBN 978-952-255-685-1.

Avainsanat: sorrutuskoe, stabiliteetti, ratapenger, instrumentointi, monitorointi, huokospaine

Tiivistelmä

TTY ja RHK (nykyisin Liikennevirasto) suorittivat Salon Perniössä lokakuussa 2009 täysimittaisen ratapenkereen sorrutuskokeen. Kokeen tarkoituksena oli kerätä kattavasti mittausdataa sortumasta ja siihen liittyvistä ilmiöistä. Tätä dataa on tarkoitus käyttää erilaisten stabiliteettilaskentamenetelmien kehittämiseen. Lisäksi kokeessa testattiin erilaisten mittausinstrumenttien teknistä soveltuvuutta stabiliteetiltaan heikkojen penkereiden monitorointiin.

Kokeessa rakennettiin savimaalle matala ratapenger vanhan, käytöstä poistetun pistoraiteen paikalle. Penkereen päälle sijoitettiin neljä 12 metriä pitkää palkistoa, joilla simuloitiin lyhyitä telivaunuja. Palkistojen päälle sijoitettiin modifioituja merikontteja, joita kuormattiin vähitellen hiekalla.

Koealue instrumentoitiin kattavasti. Alueella oli 40 huokospaineanturia, yhdeksän inklinometriputkea (yhteensä 163 automaatti-inklinometrianturia), kaksi takymetriä monitoroimassa 27 prismaa, 9 maanpaineanturia, kolme painumaletkua ja 76 liukupinnan sijainnin mittausputkea. Lisäksi konttien painoa mitattiin palkistoihin asennetuilla venymäliuskoilla ja kallistuskulmaa kontteihin asennetuilla kiihtyvyysantureilla. Kokeesta tehtiin maastomallit laserkeilaamalla.

Kontteja kuormattiin kahtena koepäivänä. Kuormituksen aikana siirtymät ja huokospaineet kasvoivat melko lineaarisesti. Muutosten nopeus alkoi kasvaa eksponentiaalisesti noin 2,5 tuntia ennen sortumaa, kuormituksen loppuvaiheessa ja sen loputtua. Lopullinen murtokuorma vastasi 87 kPa kuormaa penkereen päällä (218 kN/m junakuorma).

Muodostunut, pituussuunnassa noin 50 m pitkä sortuma oli poikkileikkaukseltaan hyvin kiilamainen. Tarkkaa liukupintaa ei saatu varsinaisesti määritettyä, kyseessä oli ennemminkin paksuhko liukuvyöhyke. Koko liikkunut savimassa häiriintyi sortumassa huomattavasti, mikä viittaa vyöhykemurtuman mahdollisuuteen.

Saven myötämisestä aiheutuva huokosveden ylipaine oli huomattavan suurta. Lisäksi huokosvedenpaineen ja muodonmuutosten aikariippuvuus oli selvästi havaittavissa. Ennen sortumaa huokosvedenpaine ja siirtymät kasvoivat jatkuvasti kiihtyvällä nopeudella ulkoisen kuorman pysyessä vakiona.

Penkereen stabiliteetin monitoroinnissa selkeimmiksi mittaussuureiksi osoittautuivat penkereen painuma ja maan sivusiirtymät sekä näitä täydentämään huokospaineiden kehittyminen penkereen keskilinjan ja alareunan alla.

Ville Lehtonen: Instrumentering och analys av ett skredexperiment på en järnvägsbank – general sammanfattning. Trafikverket, byggherreverksamhet. Helsingfors 2011. Trafikverkets undersökningar och utredningar 29/2011. 57 sidor. ISSN-L 1798-6656, ISSN 1798-6664, ISBN 978-952-255-685-1.

Nyckelord: skredexperiment, stabilitet, järnvägsbank, instrumentering, övervakning, portryck

Sammanfattning

TTU och Banförvaltningscentralen (nuförtiden Trafikverket) genomförde ett fullskala skredexperiment på en järnvägsbank i Bjärnå, Salo i oktober 2009. Syftet med experimentet var att samla data av skredet och samhörande fenomen. Datat skall användas för att vidare utveckla olika beräkningsmetoder för stabilitet. I tillägg användes experimentet för att testa hur olika instrument tillämpar sig för övervakning av bankar med låg stabilitet.

En låg järnvägsbank byggdes på lera, på plats av en gammal, avlagd stickspår. På banken placerades fyra 12 m långa bjälklag som simulerade korta vagnar med boggier. På bjälklagen placerades modifierade containrar som gradvis lastades med sand.

Försöksområdet instrumenterades omfattande. I området placerades 40 portrycksensorer, 9 inklinometer (med tillsammans 163 automatiska inklinometersensorer), två robotiska takymetrar som övervakte 27 prismor, 9 jordtrycksensorer, tre sättningslangar och 76 mätningspipor för glidytans läge. Dessutom vägde man containrars vikt med töjningsgivare och mätte deras lutningsvinklar med accelerationssensorer. Mättning av terrängmodeller gjordes med lasersvepning.

Containrar lastades i två dagar. Under lastning ökade förskjutningarna och portrycken relativt linjärt. Förändringarnas fart började öka exponentiellt ungefär 2,5 timmar före raseringen, på lastningens sista tamp och därefter. Slutlig brottlast på banken fanns 87 kPa som motsvarar 218 kN/m tågbelastning.

Den 50 m lång rasering som bildats hade en kilformig genomskärning. En precis glidyta kunde inte bestämmas, men snarare en det tjock glidzon. Den hela lermassan som var i bevegelse blev betydligt störd i raseringen, vilket pekar på ett zonbrott.

Portryck som förorsakades av flytning i leran var märkbart högt. Utöver var tidsberoendet av portrycksökning och deformationer uppenbar. Innan rasering ökade portrycket och deformationerna på en accelererande hastighet samtidigt som belastning var konstant.

De tydligaste mätbara fysikaliska storheter för bankstabilitet visade sig vara bankens sättning, jordens biförskjutning och som komplement utvecklingen av portryck under bankens mittlinje och underkant.

Foreword

This publication is an updated summary of the author's Master's thesis (Lehtonen 2010). Since the publishing of the original thesis, certain findings of the analysis have been slightly revised.

The experiment discussed here is part of a joint project between the Rail Department of the Finnish Transport Agency and the Institute of Earth and Foundation Structures at Tampere University of Technology. The project RASTAPA (run time 2009–2013) aims to improve stability calculation methods and find suitable means of improving embankment stability.

Helsinki, June 2011

Finnish Transport Agency
Construction Management

Table of Contents

1 Preface

A large part of the Finnish railway network is situated in areas of clay or peat. Soft subsoils coupled with high embankments (generally required in cold climates to avoid frost heave) can result in very low embankment stability. While there are many different ways of improving stability (e.g. counter faces, soil reinforcement, slab foundations on piles, etc.), accurate and reliable stability calculations are needed to assess the need and suitability of such solutions.

The determining loading situation for a railway embankment is a train stopped on the tracks. This results in an instantaneous application of a heavy external load and can be considered a truly undrained situation for soft soils. However, there is not much data available on such full-scale failures. Most test embankments brought to failure have been gradually constructed during a period of weeks to even years (Leroueil et al 1978) and do not, therefore, truly represent the problem at hand. Yet another factor differing from most previous experiments is that a properly designed railway embankment would rarely fail under its own weight or a widely distributed load. Instead, the loading causing a hypothetical railway embankment failure is a very narrow, intensive strip load.

There is also growing interest for undrained effective stress stability calculations. Correct approximation of pore water overpressure is essential for accuracy and reliability when using effective strength parameters. Again, there is fairly good information available on undrained pore pressure response under gradually built embankments (e.g. Leroueil et al 1990). However, the effects of very fast loading on pore pressure generation (time-dependency) in situ are unclear.

Determining the arrangement and quantity of instrumentation best suited for monitoring the stability of existing railway embankments was also of interest. Many existing embankments have a very low factor of safety, and being able to detect possible signs of an impending failure is very important.

In light of this, the Finnish Transport Agency together with Tampere University of Technology (TUT) decided to conduct a full-scale embankment failure experiment simulating a heavily loaded train coming to a standstill on a track on soft soil. The goals of the experiment were twofold:

- To gather data on a full-scale failure representing the actual design conditions. The main points of interest were pore pressure development, the nature of the failure mechanism and displacements at different phases. The data will be used for developing improved FEM and LEM calculation methods and improving common stability calculation procedures.
- To test the suitability of different instruments for monitoring embankment stability, determining the best measurable quantities and effective placement of instruments.

2 Test site and soil properties

2.1 General description

The experiment was conducted in Salo, near the southern coast of Finland. The site is situated near the edge of a marine clay area, an old, disused section of a blind track that used to serve a grain silo (Figure 1). The local topography is typical of southwestern Finland with fairly thick soft clay deposits alternating with hills of bedrock and moraine. The initial surface elevation of the site was about +8 m, the lowest point in the vicinity being a river bed at +4 m (some 100 m to the east from the site).

The blind track was built in the 1960's, but had been disused since the 1980's. It had previously been connected to the Helsinki–Turku railway, which runs nearby to the east between the site and the river. The blind track had virtually no embankment, but was built directly onto a sandy fill layer.

Figure 1 *The site before the experiment, view toward south. (Lehtonen 2010 p. 24)*

2.2 Soil properties

Several soil investigation and sampling programmes were carried out in the summer of 2009. Soil layers were determined using the Nordic weight penetration test and CPTU soundings. Undrained shear strength of clay layers was determined with in situ vane tests and fall cone tests on undisturbed samples. Constant rate oedometer tests as well as triaxial CIU and CK_0U tests were also performed.

A surface layer of sand is followed by a dry crust, a soft clay layer, clayey silt, sand and dense moraine. The clay layer grows thicker towards the east, being about 20 m thick near the river. Soil layer thicknesses and properties vary slightly in the area. The soft clay layer turns thicker towards the east (towards the centre of the large clay area). The clay layer was thinnest in the northern part of the test area, where it was about 3.5 m thick. The soft clay in the middle was about 4 m thick under the track and 4–-5 m thick along the side. Thickest fill was found under the old track, where it was about 1.5 m – elsewhere in the test area the layer was about 1 m or less.

General soil properties and sounding results are shown in Table 1 and Figure 2. There was fairly wide scatter between corresponding measurements on many properties, although the general trends were apparent.

Table 1 *General soil properties in the test area. Su values are reduced according to Finnish guidelines, based on liquid limit.*

	γ [kN/m^3]	s_u [kPa]	φ' [°]	w [%]	w_L [%]	POP [kPa]	sensitivity
Fill (sand)	18…19			10			
Dry crust	16	>20 (*		40			
Soft clay (level +2…+6 m)	15…16	9…20(**	25	60…90(***	50…80(***	~20	~40
Clayey silt	17…18	20…30	27	30…60	30…40	20…30	~40

(* Non-reduced ("small-scale") vane shear strength in the dry crust was well over 50 kPa
(** Undrained shear strength increased with depth (~1 kPa/m)
(*** Water content was generally above the liquid limit. Water content measurements had large scatter.

The soft clay was slightly overconsolidated, fairly plastic and quite sensitive. The clay fraction of the soft clay varies between 40% and 70%, the largest clay fraction being in the middle of the layer.

The fill under the track was mostly uniformly grained sand (d_{50} = 0.3 mm), while elsewhere it was a fairly non-homogenous mixture of rocks (d < 300 mm), sand and clay.

At the time of the experiment, the hydrostatic ground water level was at about +7 m.

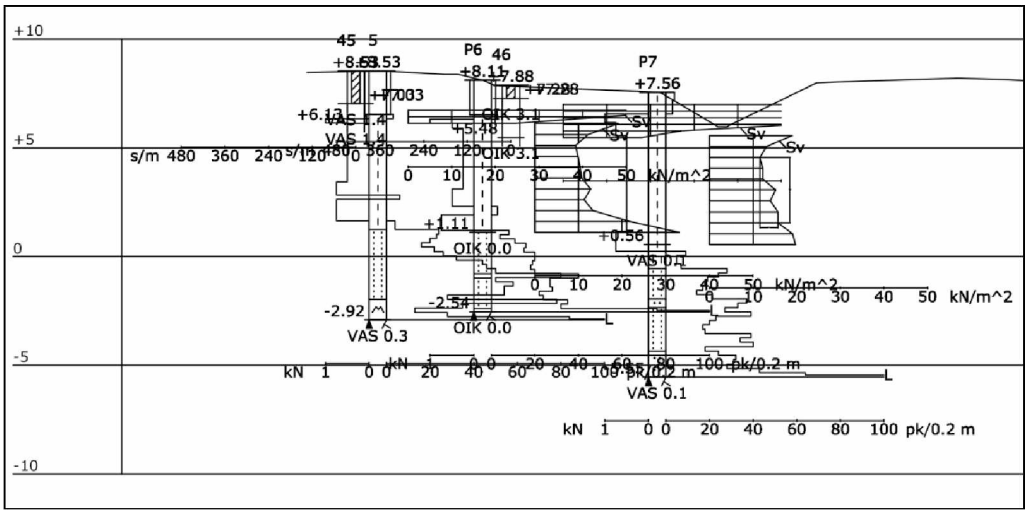

Figure 2 *Nordic weight penetration test and vane shear test diagrams from the center of the test area. Soil surface shown after cutting and excavating the ditch. (Lehtonen 2010 p. 26)*

3 Experimental arrangements

3.1 General arrangements

To ensure a controlled failure, the inherent stability of the embankment was reduced by changing the cross-section geometry (Figure 3). A small embankment (h = 0.6 m, L = 60 m) was built in place of the old track, which was removed. A new track with concrete sleepers and K60 rails was built on the new embankment. To reduce stability and to control the slip surface location, a 2 m deep ditch was excavated (bottom at level +6 m, at a horizontal distance of 14.5 m from the embankment centreline). The ditch location was chosen based on initial calculations about the most likely slip surface, with the intention that the eventual slip surface would end at the bottom of the ditch. To further reduce stability, the ditch was kept dry during the actual experiment with a submerged pump. The top soil between the embankment and the ditch was removed to a depth of 0.3–0.6 m. The cut soil mass was placed as a small counter face behind the ditch to help contain the failure.

Figure 3 *Site after geometry change. The embankment is yet to be constructed in the upper left corner of the picture.*

A train (Figure 4) was simulated by four steel frameworks, each 12 m long. The frameworks consisted of transverse beams to simulate bogie carriages and longitudinal beams to support containers, which were gradually filled with sand. Each framework ('car') carried four modified sea containers in two tiers. The bottom containers had had their tops removed, while the top containers had had both their tops and bottoms removed. This way both container rows could be set in place before commencing the loading, which was done through the top containers. All containers were reinforced with horizontal steel bars running through them to brace against the earth pressure from the sand load.

The beams used in the frameworks were fairly large: an HE200B I-beam as the longitudinal ones and an HE300B as the transverse ones. The beams were also stiffened with extra steel plates in places where large shear stresses would occur.

Figure 4 *Site before loading. The ditch was drained of water prior to the start of loading. (Lehtonen 2010 p. 71)*

The loading was performed using a telescopic conveyor belt. The conveyor belt could reach every container from a single position that was far enough for safety in case the containers would tip over during loading. The loaded soil masses were weighed by the front loader used to load the sand into the conveyor belt feeder. This was doubled by weighing the containers by strain gauges installed in the frameworks. In addition, the conveyor belt had a down-looking video camera for visually observing sand distribution in the containers.

The load cycles during the experiment were such that the two middle 'railway cars' were loaded first and the two outermost cars last. During the initial stages the middle cars were loaded more heavily by (5 kPa) than the outermost cars in an attempt to ensure that the failure would commence in the mid part of the area. Based on the car numbering of Fig. 5, the loading sequence was 3—2—1—4.

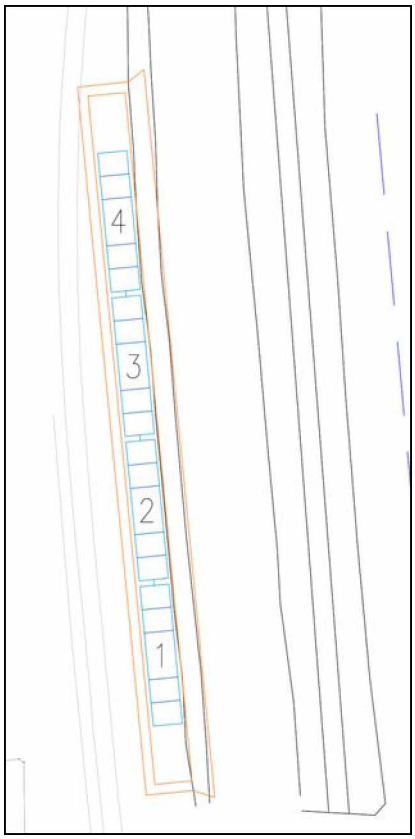

Figure 5 Car numbering. (Lehtonen 2010 p. 17)

During one loading cycle each car was generally loaded with 15 tons/cycle. As the length of a single framework is 12 m, spacing 0.5 m and sleeper length about 2.5 m, a 15 t load is roughly equivalent to a 4.8 kPa homogenous area load. The loading under a given car is calculated as:

$$q_i = \frac{G_i + G_{cont} + G_{fw}}{12{,}5m \cdot 2{,}5m} \quad (1)$$

where

q_i = Area load under car i [kPa]
G_i = Weight of the soil loaded in a given car [kN]
G_{cont} = Dead weight of the containers on the framework, ca. 90 kN
G_{fw} = Dead weight of the framework, ca. 35 kN

3.2 Instrumentation

3.2.1 General issues and placement guidelines

The goals of the instrumentation were both to gather extensive data on the physical phenomena occurring during the experiment and to test the monitoring capabilities of the instruments themselves (functioning, best placement, etc.). Many measurements were doubled with different methods both to ensure the gathering of data in case of instrument failure and to be able to compare the accuracy and suitability of different methods.

Hunter & Fell (2003) suggest that generally good quantities indicating an impending failure are:

- vertical deformation at and beyond the embankment toe
- lateral surface deformation at the embankment toe
- lateral deformation with depth at the embankment toe
- excess pore pressure under the embankment and close to the failure zone

They also state that vertical deformation under the embankment centreline is generally not a good indicator of low stability, since it does not usually remain in the failure zone. However, the test embankments examined by Hunter & Fell were notably higher and wider, and they failed under their own dead weight. In contrast, a railway embankment is usually fairly low and subject to a highly concentrated external load. There one would expect a failure mechanism where the failure zone starts behind the sleepers (which act as reinforcement on the surface) and proceeds fairly steeply downwards. Therefore, embankment settlement was considered a viable indicator of low stability in this case.

In addition to deformation and pore pressure measurements, vertical earth pressure was measured. The "axle geometry" of the frameworks was fairly evenly distributed, representing short cars with bogies. Thus the vertical load in the soil could be considered fairly homogenous. Earth pressure transducers could be used to test the validity of this claim. They could also be used for estimating the change in general distribution of vertical stress at depth.

After careful consideration, it was decided that measurement of the following quantities in the failure experiment would serve the aforementioned purposes:

- Excess pore pressure along the most likely failure zone (pore pressure transducers)
- Settlement under the upper edge of the embankment (settlement tubes)
- Vertical deformation from the failure side embankment toe to the edge of the ditch (settlement tubes, total stations, metering points)
- Lateral deformation of the surface, from the toe to the ditch (total stations, metering points, inclinometers)
- Lateral deformation of the soil, from the toe to the ditch (inclinometers)
- Vertical earth pressure under the embankment centreline (earth pressure transducers)
- Tilting of the cars (acceleration gauges)
- Slip surface location (inclinometers, vertical tubes)

In addition, the following "secondary" measurements and observations were made during various phases of the experiment:

- Weighing of the soil loaded in the containers (weighing front loader, strain gauges)
- Measurement of input voltage of various analog instruments (needed for correct instrument calibration)
- Measuring of surface models and instrument location measurements at various stages (VRS-GPS, total stations, laser scanning)
- Climate measurements (air temperature, atmospheric pressure)

Locations of key instruments are shown in Figure 6.

All data from analog transducers (pore pressure transducers, earth pressure transducers, strain gauges, acceleration gauges) were collected with data loggers and stored on computers. Digital data (total stations, settlement gauges) was stored directly on computers. The inclinometers had their own data storage units, from where the data was wirelessly transferred to a remote server for viewing.

Some monitoring equipment were ready-made, off-the-shelf products, while some were designed and built at TUT's Institute of Earth and Foundation Structures.

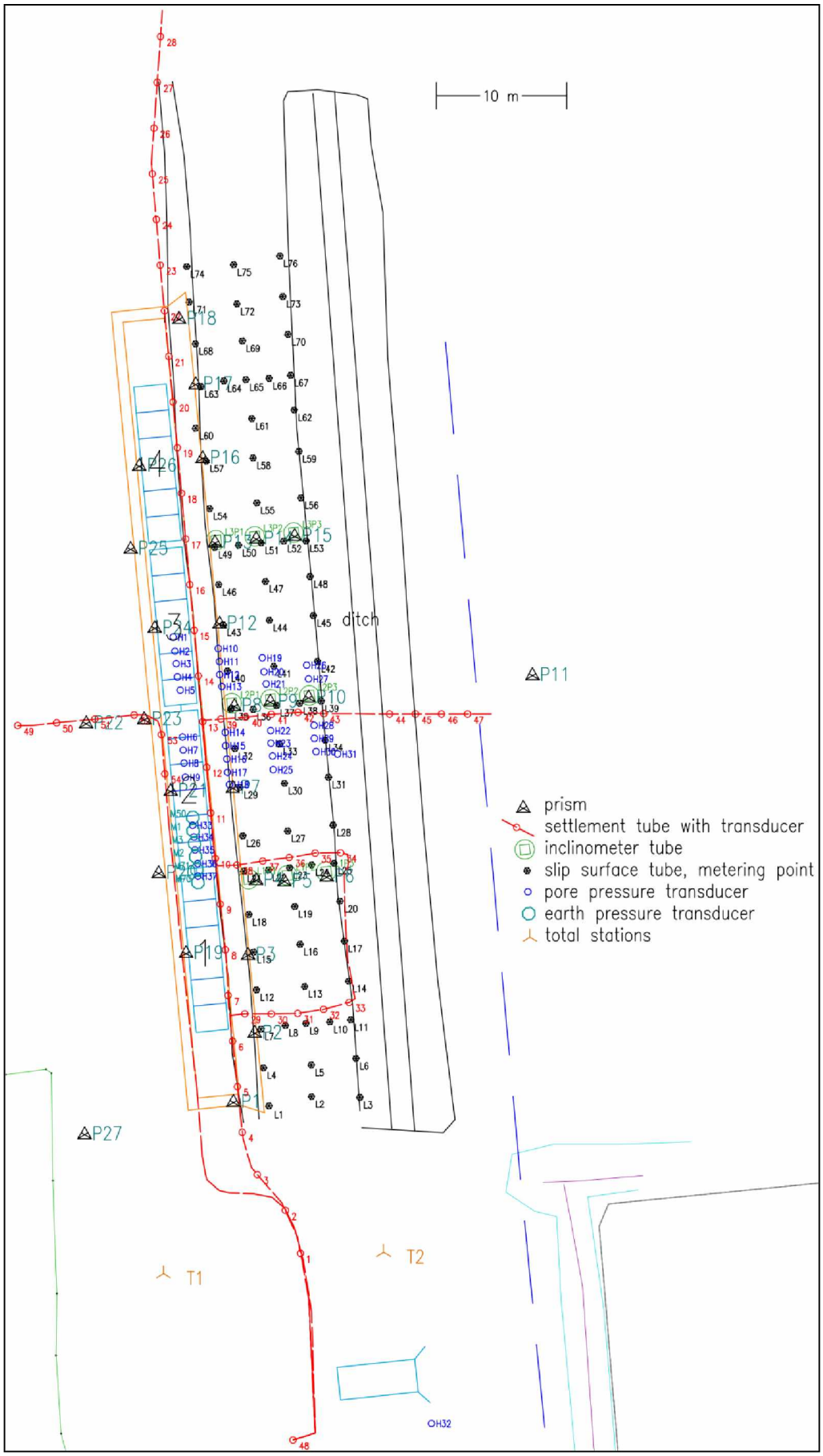

Figure 6 *Locations of key instruments.*

3.2.2 Pore pressure transducers

A total of 37 strain-type pore pressure transducers (Figure 7) were used in the experiment. They are off-the-shelf equipment intended specifically for measuring pore water pressure in soils. They have a conical tip for pushing them into the soil, and a porous stone in front of the membrane to isolate pore water pressure from earth pressure.

Figure 7 *A pore pressure transducer. The end of the device has a thread-fastened bushing which fits a rod used to push the transducer into the soil. When the transducer is at a desired depth, the rod is pulled back up, leaving the transducer in place. The cable is used to recover the transducer after the experiment. (Lehtonen 2010 p. 41)*

The governing idea in their placement was to measure excess pore water pressure especially in the failure zone (which would show considerable excess pressure due to yielding). Thus most transducers (H1–H31) were grouped in the middle of the area around the most likely failure surface (based on calculations) mainly in four lines (Figure 8). The transducers in each line were installed at 0.25 m depth intervals. To minimise the effect of soil disturbance, the transducers were set at least 1 m apart horizontally.

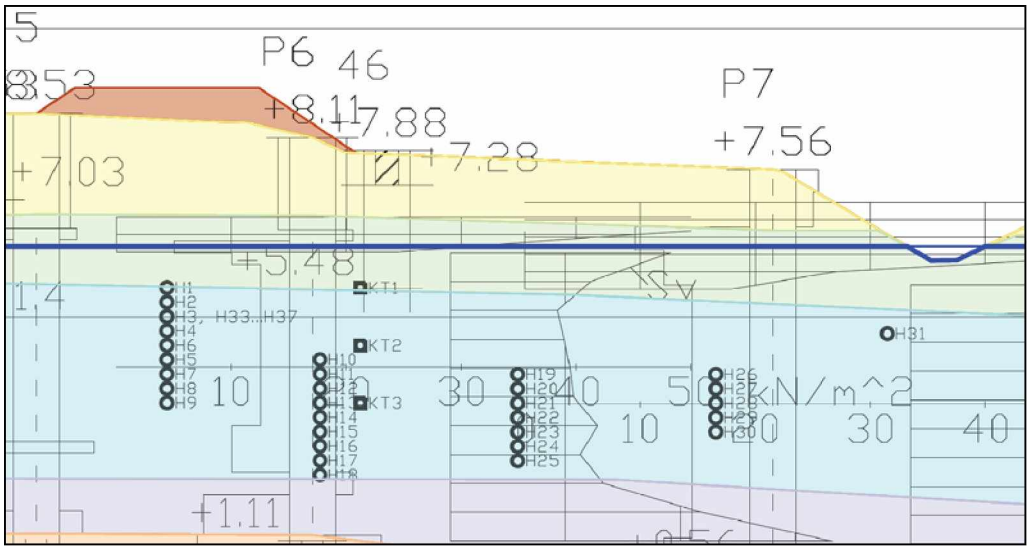

Figure 8 *Cross-section of pore pressure transducer placement (Lehtonen 2010 p. 33)*

In addition to the 31 "failure zone" transducers, five others (H33–H37) were installed under the embankment centreline at height level +5.0 m (4 m under the embankment), 1 m apart from each other. Together with earth pressure transducers at similar locations (at +7.5 m) they were used to observe longitudinal irregularities in stress changes induced by the axle geometry of the frameworks. An extra transducer (H32) was installed outside the test area for reference.

Each pore pressure transducer was tested in laboratory conditions beforehand, the calibration coefficients and constants being set according to the official calibration reports. They were installed two weeks before the actual experiment to allow the dissipation of excess pore pressure from installation. The porous stones were de-aerated on site using a vacuum pump right before installation to ensure proper functioning.

3.2.3 Settlement tubes

A settlement tube is a horizontal fluid-filled flexible plastic tube containing pressure transducers. If one end of the tube is held at a constant elevation, and other parts move freely as the soil deforms, the settlement at a given point can be calculated based on the change in hydrostatic fluid pressure. The concept is not entirely new, but most existing applications have only one movable transducer, which makes it difficult to monitor large areas constantly and automatically. In addition, the transducers often measure pressure relative to atmospheric pressure. The need of an air pressure tube connected to the transducer would limit the length of such a tube. (Luomala 2010)

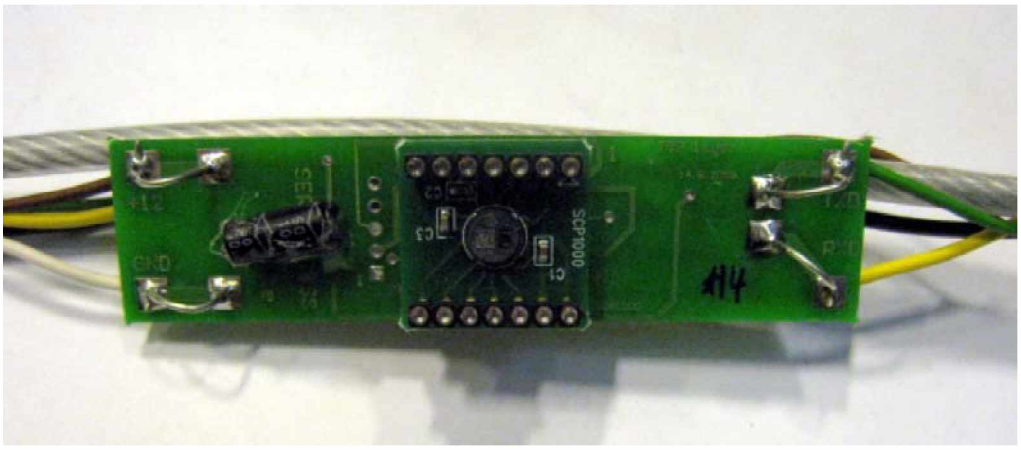

Figure 9 *The pressure transducer used in the TUT settlement tube (Luomala 2010 p. 28)*

A considerably improved settlement tube concept has been developed at TUT's Institute of Earth and Foundation Structures. Several small digital pressure transducers (Figure 9) are installed inside a tube at given locations. The transducer locations and spacing within the tube can be chosen freely. The transducers can be programmed to automatically measure a pressure reading at given time intervals. These readings can then be stored in a database and connected to a monitoring alarm system if needed. The transducers measure absolute pressure, which eliminates the need for a separate tube for atmospheric pressure. By installing one transducer in the fixed part of the tube and comparing readings of all other transducers to its readings, the effect of atmospheric pressure changes is eliminated, since a change in external air pressure affects every transducer in the fluid equally.

The fluid used in the tube needs to be non-conductive, non-corrosive and it must not freeze or vaporise in the operating conditions. The TUT settlement tubes use biodegradable hydraulic fluid, which satisfies all these requirements in Finnish conditions.

Environmental temperature has an effect on the transducers' pressure readings. Therefore, the transducers also measure temperature and make corrections accordingly before giving the pressure reading. (Luomala 2010) Proper installation of the tubes deep enough into the soil helps keep the temperature constant and also reduces the chance of damage to tubes due to external forces.

TUT's improved settlement tube can simultaneously monitor effectively settlements over a distance of several hundred metres if need be. Thus the instrument is especially suitable for monitoring railway or road embankments. The length of a tube is limited by the fact that it needs to be pulled straight for the installation of the transducers, and that long tubes are generally difficult to handle.

The transducers were assembled and installed in the tubes beforehand at the TUT workshop. On site the tubes had only to be laid down (Figure 10), filled with oil and the wiring connected to a computer before commencing measurements. The tubes were installed in 30—50 cm deep excavations in the sandy fill layer. The tubes must not be allowed to remain in direct contact with jagged particles (e.g. crushed rock aggregate), so as to prevent damage to them.

Figure 10 *Settlement tube before covering. Transducer locations were marked with yellow tape and their co-ordinates were measured before covering the tube. Image by Kauko Sahi.*

Three tubes were used in the failure experiment: the longest one (≈110 m, 28 transducers) was installed under the failure side top edge of the embankment, and it extended beyond both ends of the embankment. The second tube (≈65 m, 19 transducers) was installed in three transverse cross-sections between the embankment and the ditch, with one end extending over the ditch (a short section of the tube that ran over the ditch was exposed). The third tube (≈70 m, 6 transducers) was installed under the opposite top edge along half of the embankment, and its end was brought 10 metres away from the embankment. Note that the tubes did not have transducers along their entire length; transducers were installed only in locations useful for the experiment. In addition to the transducers in the tubes, one (number 48) was placed outside the area to measure atmospheric pressure and temperature.

The transducer locations are shown in Fig. 6.

The reference transducer used in the analysis was number 1 in the first tube. The operating conditions of the transducer were considered stable, since it was located well outside the assumed failure area and installed in the ground where temperature is constant.

3.2.4 Total stations

Two robotic total stations were used to automatically monitor surface displacements during the experiment. The total stations were specifically designed for automatic monitoring purposes. The units used in the experiments have a given angle measuring accuracy of 0.15 mgon and range accuracy of 0.6 mm + 1 ppm, which can be considered very accurate. The total stations are controlled by a commercial software from the instrument manufacturer. The monitoring routine is set in the program, and the measurements are stored in a database.

The total stations were placed on the edge of the area so that one covered the failure side and the other the back side. 18 passive miniprisms (P1–P18) were installed on the failure side, five in the ground on the opposite side (P20, P22, P23, P25, P27) while four were installed on the lower containers, one per car (P19, P21, P24, P26). In addition, three reference prisms were installed on the walls of surrounding buildings. They were used for orientation of the total stations (both for monitoring and other surveying purposes), and to indicate any shifting of tilting of the total stations. The programmed monitoring routine included an hourly check of the locations of the monitoring total stations.

The prisms on the soil surface were installed using steel rods that were pushed or hammered firmly into the soil. The prisms were installed as close to the surface as possible to reduce the effect of the rod possibly tilting (the purpose being to measure the displacement of the soil surface, not of the prism itself).

Total stations were also used for measuring the locations of various instruments during installation and for general soil surface mapping before and after the experiment.

3.2.5 Inclinometers

Nine automatic inclinometers were used to measure displacements in the soil. They were commercial units made by FinMeas Oy. The inclinometer tubes contained several fixed inclination transducers eliminating the need to periodically move a single transducer as is often the case. The resolution of the inclination profile depends on the number of transducers per unit length of tube.

The inclinometer tubes were installed between the embankment and the ditch in three transverse lines of three tubes, each line located laterally to the gap between cars (see Fig. 6 for locations). The tube bottoms were installed in the dense sand/moraine layer, the bottom depth varying from 8 to 9.5 m (elevation -2 to +0 m). Eight tubes had inclination transducers with a spacing of 0.5 m, while tube L3P2 had a spacing of 1.0 m.

The used inclination transducers were biaxial units, measuring both transverse and longitudinal inclination. Coupled with every inclinometer tube was a data acquisition unit used both for storing data and transmitting it wirelessly to a remote server for near-real-time viewing.

3.2.6 Earth pressure transducers

Earth pressure transducers designed and built at TUT's Institute of Earth and Foundation Structures (Figure 11) were used to measure the longitudinal distribution of vertical stress under the embankment. The transducers differ from most commercial units by their large size (d = 384 mm), which helps reduce the effect of soil vaulting above the unit, especially when installed in coarse-grained soils.

Earth pressure measurement is based on the compressive strain imparted on a steel core inside the unit. The strain is measured with strain gauges attached to the core. The data produced by the unit is analog and is collected with data loggers.

The transducers were installed under the embankment centre in the sandy fill layer, at an elevation of +7.5 m.

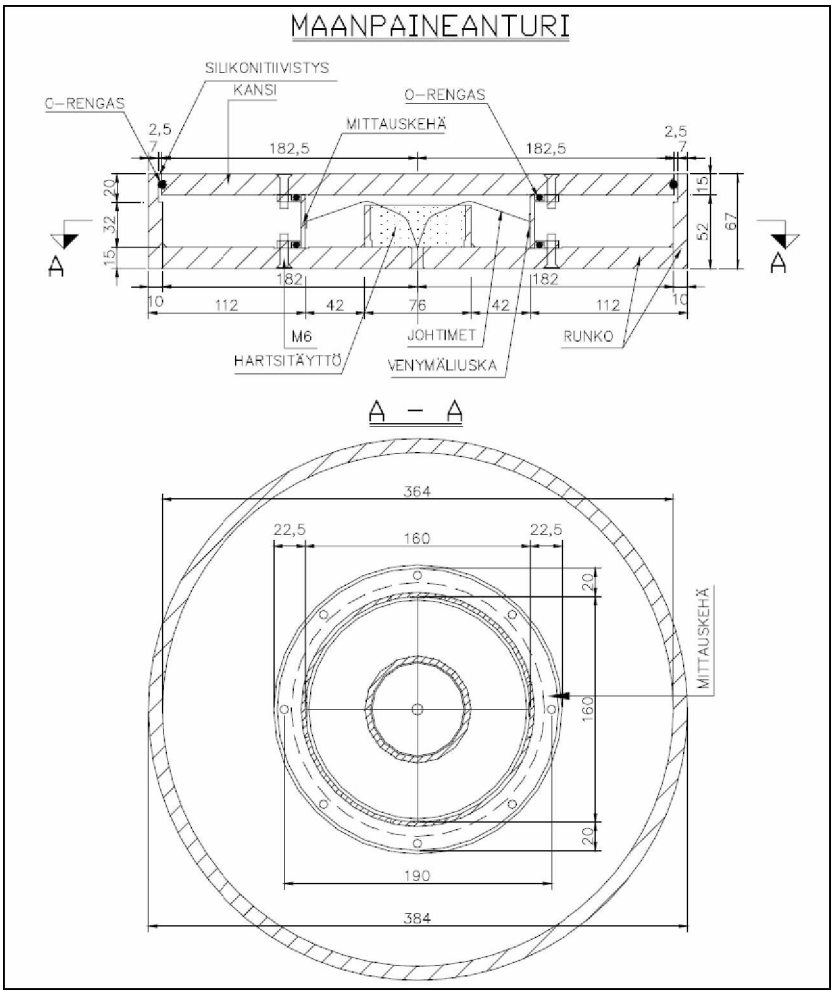

Figure 11 *(Laaksonen 2005 p. 54)*

3.2.7 Slip surface tubes

To estimate slip surface depth and the overall dimensions of the failure, flexible plastic tubing (used in electrical wiring applications, Figure 12) was installed vertically in the soil. The tubes were assumed to follow soil movements during failure and form a sharp bend at the slip surface. The depth of the bend can be measured from the surface after failure by using a wire with a rigid tip.

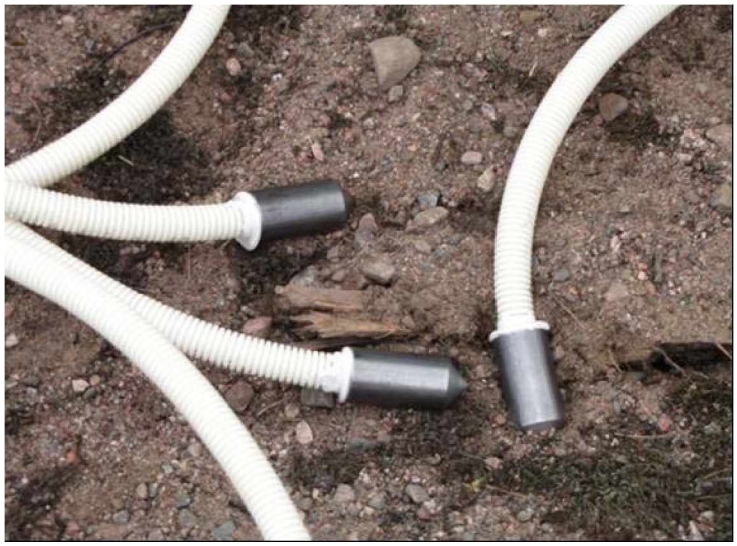

Figure 12 Slip surface measuring tubes (Lehtonen 2010 p. 52)

The tubes (a total of 76) were installed in a grid between the embankment and the ditch. A metal end piece was attached to the lower end of the tube, and a long steel rod was used to push down against the end piece. The tubes were installed as deep as pushing with manpower would allow, i.e. to the clayey silt layer.

The upper ends of the tubes were anchored to the surface with expanding polyurethane foam. After the foam had hardened, a small screw was pushed into it, thus forming 76 accurate displacement measurement points along the area. The point locations were measured before and after the failure by total stations. The tubes and points allowed estimating the extents and shape of the failure in the soil.

3.2.8 Strain gauges

The steel frameworks were instrumented with strain gauges for weighing the containers. Although the loaded soil was weighed also with the front loader, accurate data on the external load was considered so important that the measurements had to be doubled.

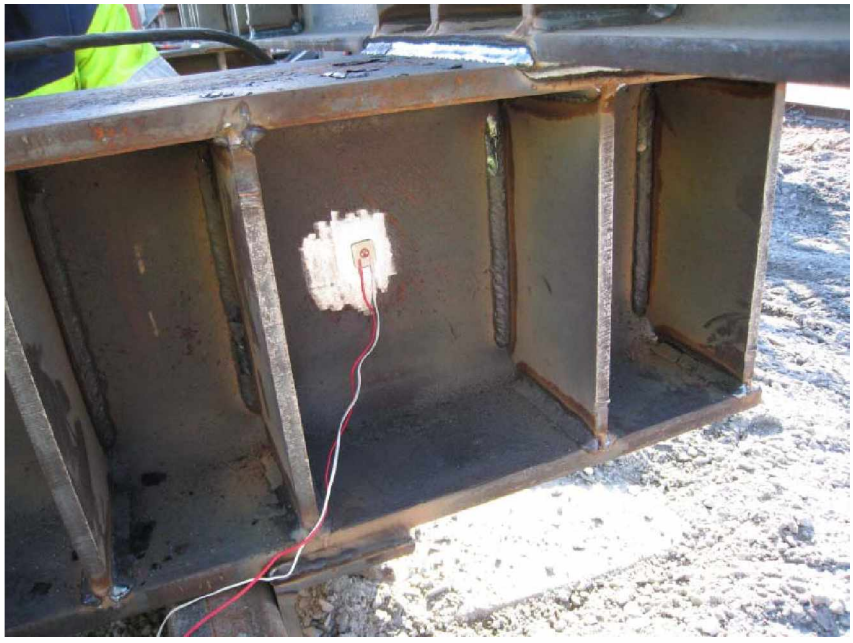

Figure 13 *Instrumented beam. Note the stiffening plates needed to avoid buckling of the beam web. (Lehtonen 2010 p. 55)*

The transverse steel beams representing train axles were fitted with biaxial strain gauges on both sides of each "wheel" (Figure 13). The gauges measured the shear strain mobilised in the beam web between the rail and the longitudinal beam. From this strain the loading of each "wheel" could be calculated.

All strain gauges were calibrated on site with a hydraulic jack containing a force transducer. The jack loaded the beams in a manner comparable to the external load from the containers.

4 The experiment

The experiment was commenced on 20 Oct. 2009. All preparations had been finished by then. Most of the measurements were started some hours before loading was commenced.

Loading started at 15:55 and continued until 18:49 (Table 2). As the daylight period in Finland in late October is rather short (darkness begins to set at around 17:00), the loading was stopped for the night at 24 kPa in the middle cars and 21 kPa in the outer cars. It was hoped that the eventual failure would occur during daylight the next day. All automatic monitoring equipment was left running for the night, but due to a software error most analog instruments (pore pressure and earth pressure transducers) stopped functioning right after the personnel left the area. The situation was noticed and rectified at 7:00 the next morning when the crew returned to the site. Total stations, settlement tubes and inclinometers functioned throughout the night.

During the night continuous transverse movement of the embankment was measured by the total stations. Pore pressure had also increased slightly during the night (even when the effect of atmospheric pressure changes is taken into account).

Table 2 External loading after load cycles.

	External load at end of cycle [kPa]			
Duration of load cycle	Car 1	Car 2	Car 3	Car 4
Start	4	4	4	4
20 Oct. 2009 15:55–16:35	6.6	9.6	9.8	6.5
16:41–17:18	11.3	14.3	14.6	11.2
17:20–17:56	15.9	19.1	19.3	15.9
18:13–18:49	20.7	23.8	23.9	20.6
21 Oct..2009 8:14–8:53	24.6	29.5	29.4	24.5
9:00–9:36	29.3	34.3	34.3	29.3
9:39–10:14	34.0	39.2	39.2	34.2
10:37–11:11	39.0	44.1	44.2	39.1
11:13–11:47	43.9	49.0	49.1	44.0
12:04–12:39	48.8	53.9	53.9	48.9
12:41–13:15	53.7	58.8	58.8	53.8
14:00–14:35	58.7	63.7	63.8	58.7
14:52–15:31	63.6	68.5	68.6	63.6
15:51–16:26	68.4	73.4	73.5	68.5
16:46–17:27	73.3	78.3	78.4	73.4
17:39–17:59	78.2	78.3	78.4	78.3
18:05–18:46	83.1	83.2	83.2	83.2
18:56–19:19	85.3	85.2	85.1	85.3
19:26–19:34	85.3	87.3	87.1	85.3

The experiment was continued after 8:00 in the morning of the second day. The load was increased fairly linearly at a rate of 5 to 7 kPa/h (cycles of 5 kPa, each cycle taking about 45 minutes). During the initial loading, pore pressure and displacements increased fairly linearly (a slightly accelerating trend was observed). After 17:30 it was decided to increase the load of the two cars at the ends to the level of the middle cars. That was done to ensure the failure, as the containers on the middle cars were

loaded close to capacity at that point. No obvious signs of an impending failure had been observed by then, other than the moderate, fairly linear pore pressure and displacement increases.

Selected excess pore pressure readings and loading in the middle cars are presented in Figure 14.

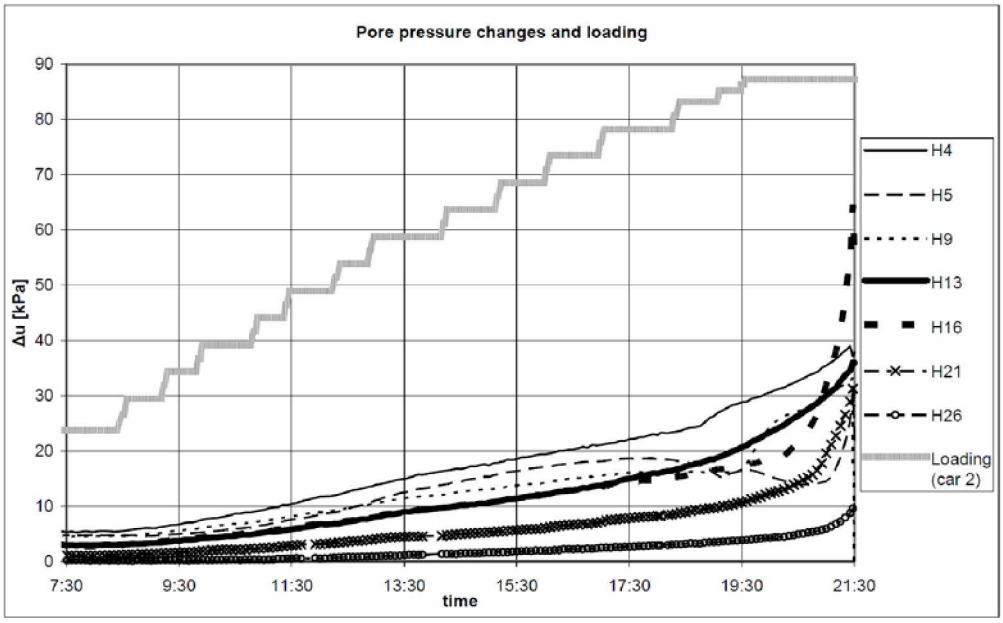

Figure 14 *Selected excess pore pressure readings and external loading during the second day.*

When the load in the middle cars reached about 78 kPa (around 18:00), some irregular pore pressure patterns began to develop. With the load at about 78 to 85 kPa, some pore pressure transducers indicated a slight drop in pore pressure (5 to 10 kPa) despite increasing load. At about 19:00, transducers under the embankment centreline and toe began to show accelerating increases in pore pressure, followed by other transducers further away after about 20:30. During the final half hour before the failure, all pore pressure transducers in the failure area indicated continuously accelerating pore pressure growth.

Loading ended at about 19:30, at which time the final load of the middle cars was 87 kPa and that of the end cars 85 kPa. The cars were filled to close to maximum height. Further loading would have been possible by adding water to the containers, but that was deemed unnecessary at that point as there were already some signs of an impending failure.

The displacement response was in general very similar to the pore pressure increase. Embankment settlement and general transverse displacement increased fairly linearly during loading (with a slightly accelerating trend), and began accelerating notably before the failure, after about 19:00.

First visual signs of the failure were the tilting of cars 2 and 1 some minutes before failure. At failure (Figure 15), cars 1, 2 and 3 quickly sunk and fell on their side away from the embankment. Car 4 fell a few seconds later after fairly little settlement compared to the others. At failure, the embankment was displaced downwards (Figure

16), while soil between the embankment and the ditch moved upwards and towards the ditch.

Figure 15 *The embankment failure. (Lehtonen 2010 p. 77)*

Figure 16 The embankment after failure. (Lehtonen 2010 p.78)

Pore pressure, inclinometer and settlement tube measurements were continued after the experiment. During the following day, the area was surveyed and the slip surface tubes were measured.

The general shape of the failure was evident from visual observations. The slip surface began behind the sleepers and ended on the bottom of the ditch. The longitudinal extents of the slip surface could be approximated from diagonal cracks on the surface. The failure mechanism consisted of two different parts: the embankment had moved down while other parts had moved up and to the side. The soil had cracked at the embankment toe, where the two soil masses had most likely moved in opposite directions vertically. Largest displacements were observed in the middle of the area. (Figures 17 and 18)

Some weeks after the failure a CPTU survey was carried out. The same survey points as in the pre-experiment survey were used. That allowed comparing the soil strength profiles before and after the experiment.

Figure 17 *Left: Cracked soil at the embankment toe. Right: Crack by the ditch in the center part of the area (spot of largest ground rise) (Lehtonen 2010 p.79)*

Figure 18 *The passive end of the slip surface. (Lehtonen 2010 p.80)*

5 Measured results

Selected results from the experiment are shown in Figures 19 to 33. The focus is on results from the second day of the experiment, as during the first day the measured changes were quite small.

5.1 Pore pressure transducers

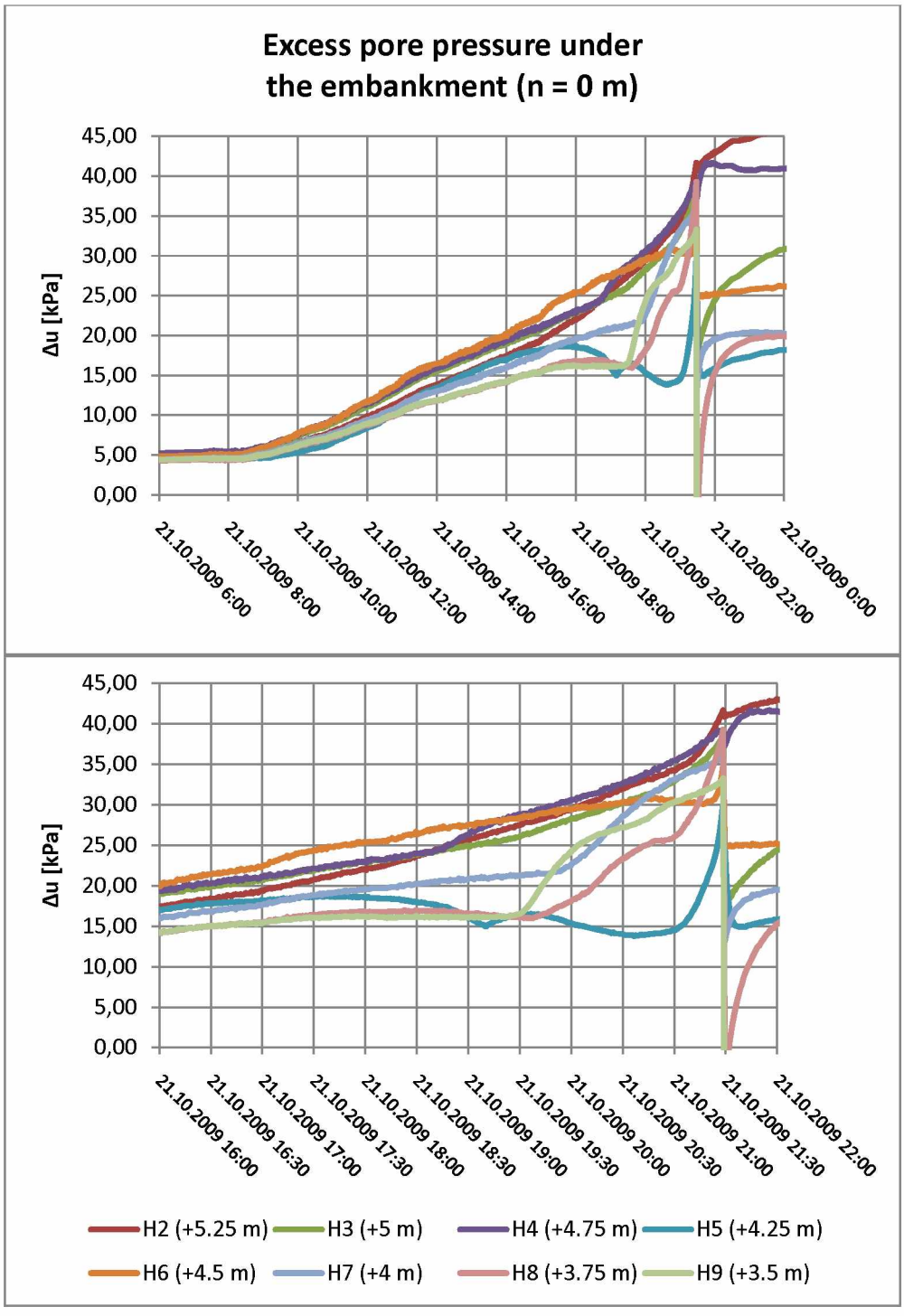

Figure 19 *Excess pore pressure under the embankment.*

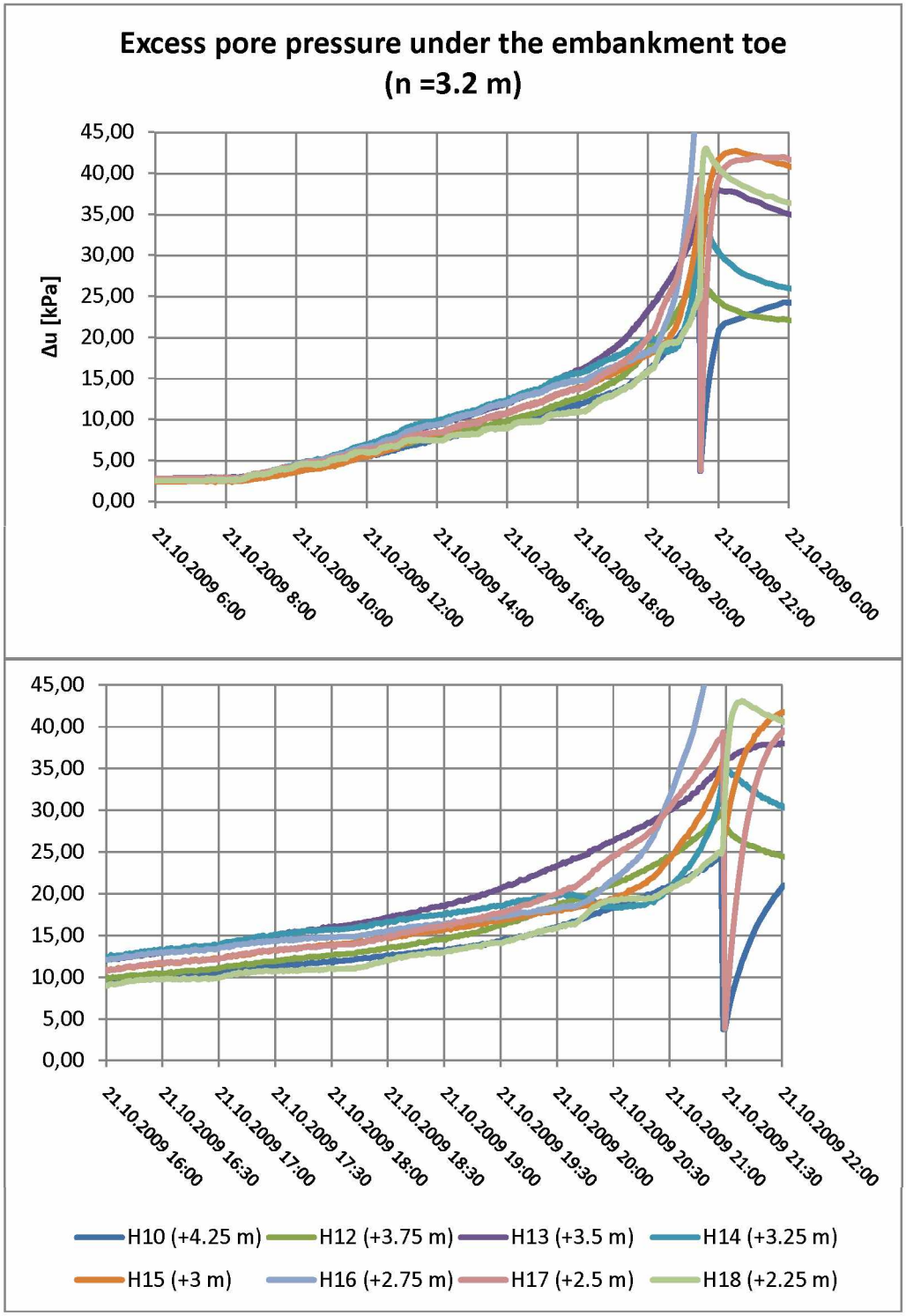

Figure 20 *Excess pore pressure under the embankment toe.*

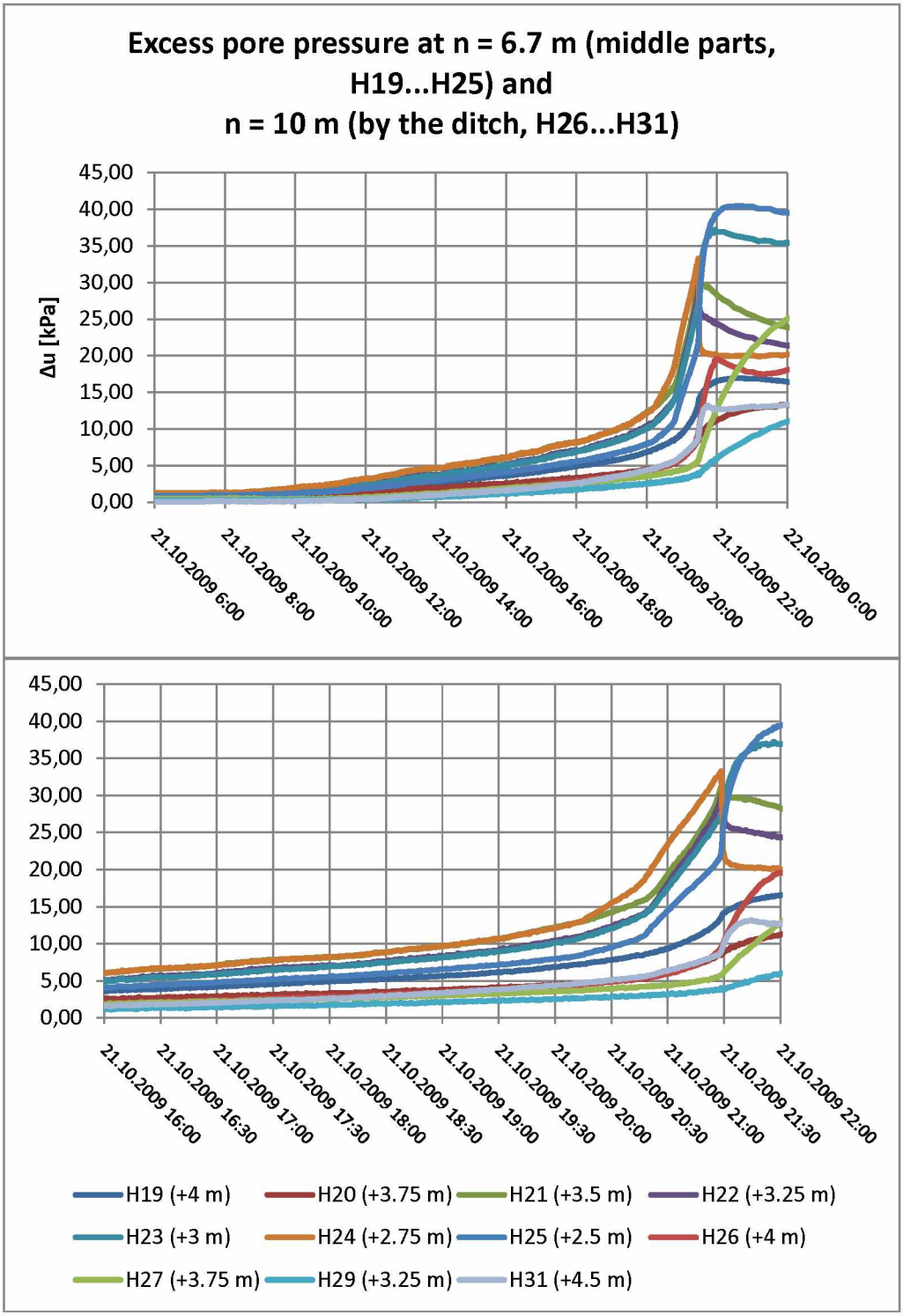

Figure 21 *Excess pore pressure between the embankment and the ditch, and next to the ditch.*

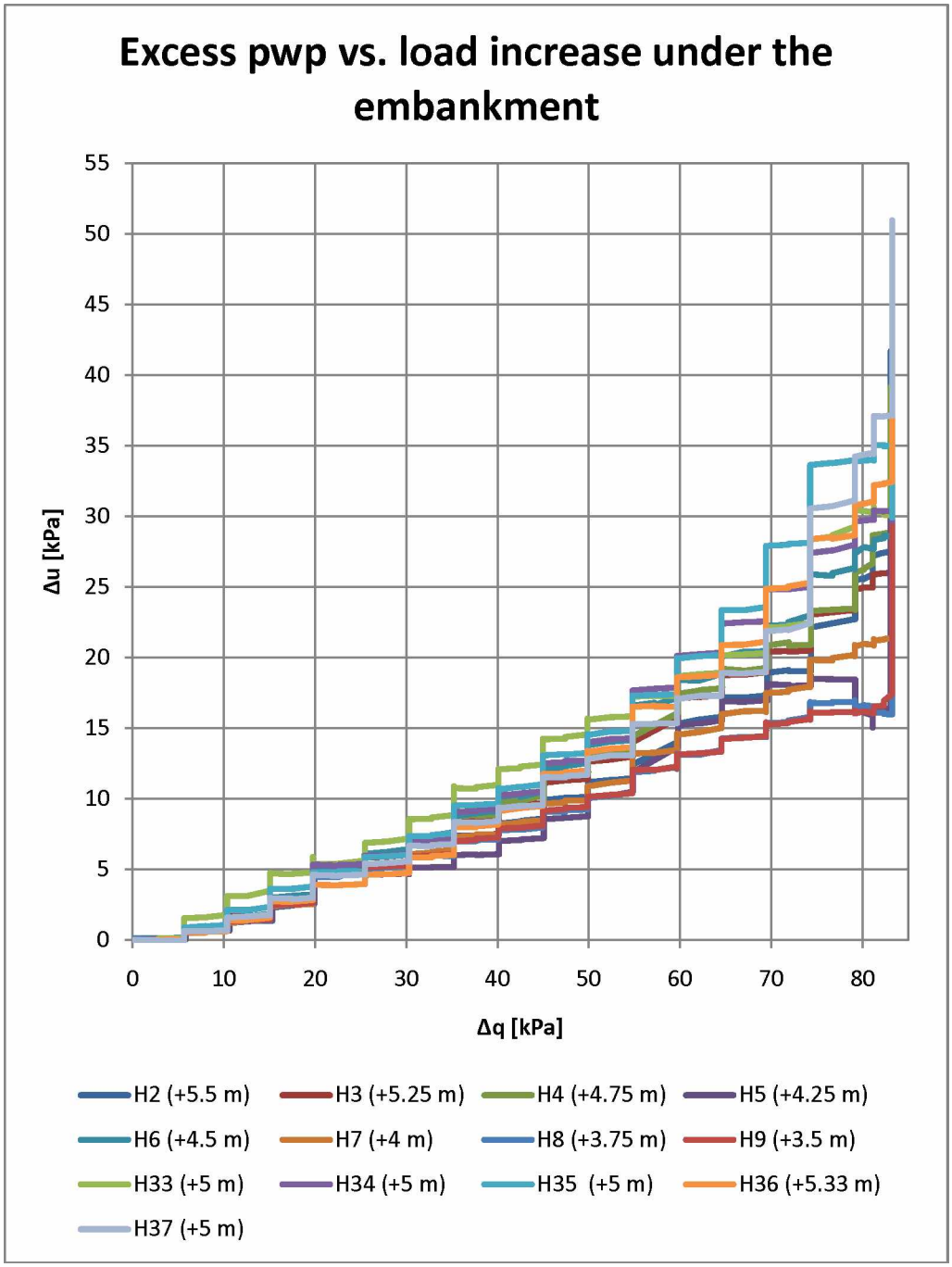

Figure 22 *Excess pore pressure as a function of external loading.*

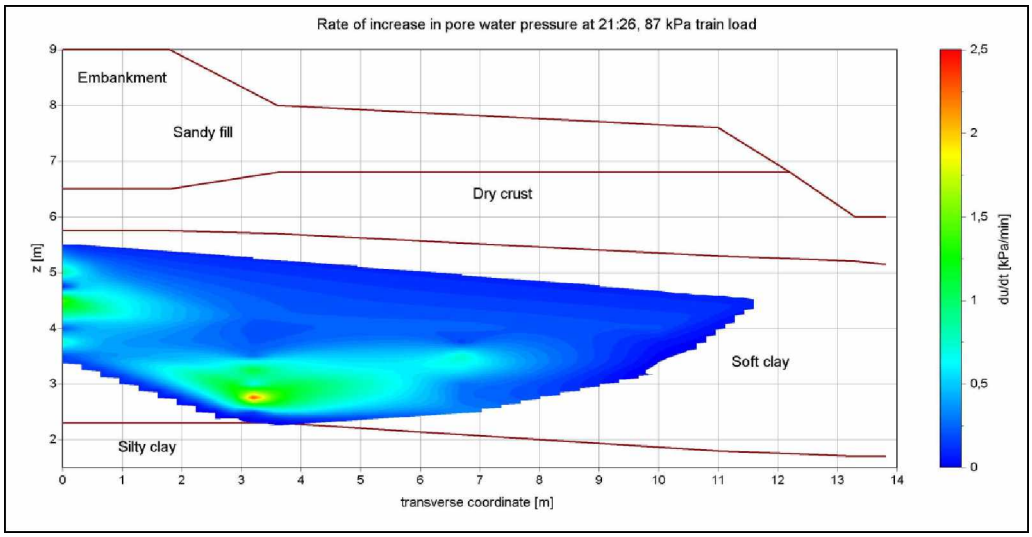

Figure 23 *Rate of pwp increase right before failure*

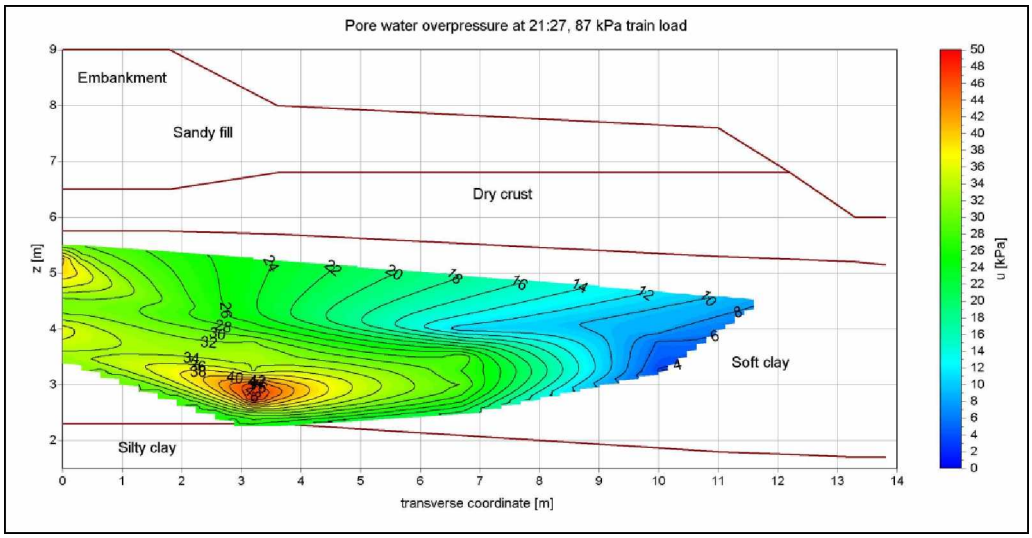

Figure 24 *Excess pwp right before failure.*

5.2 Inclinometers

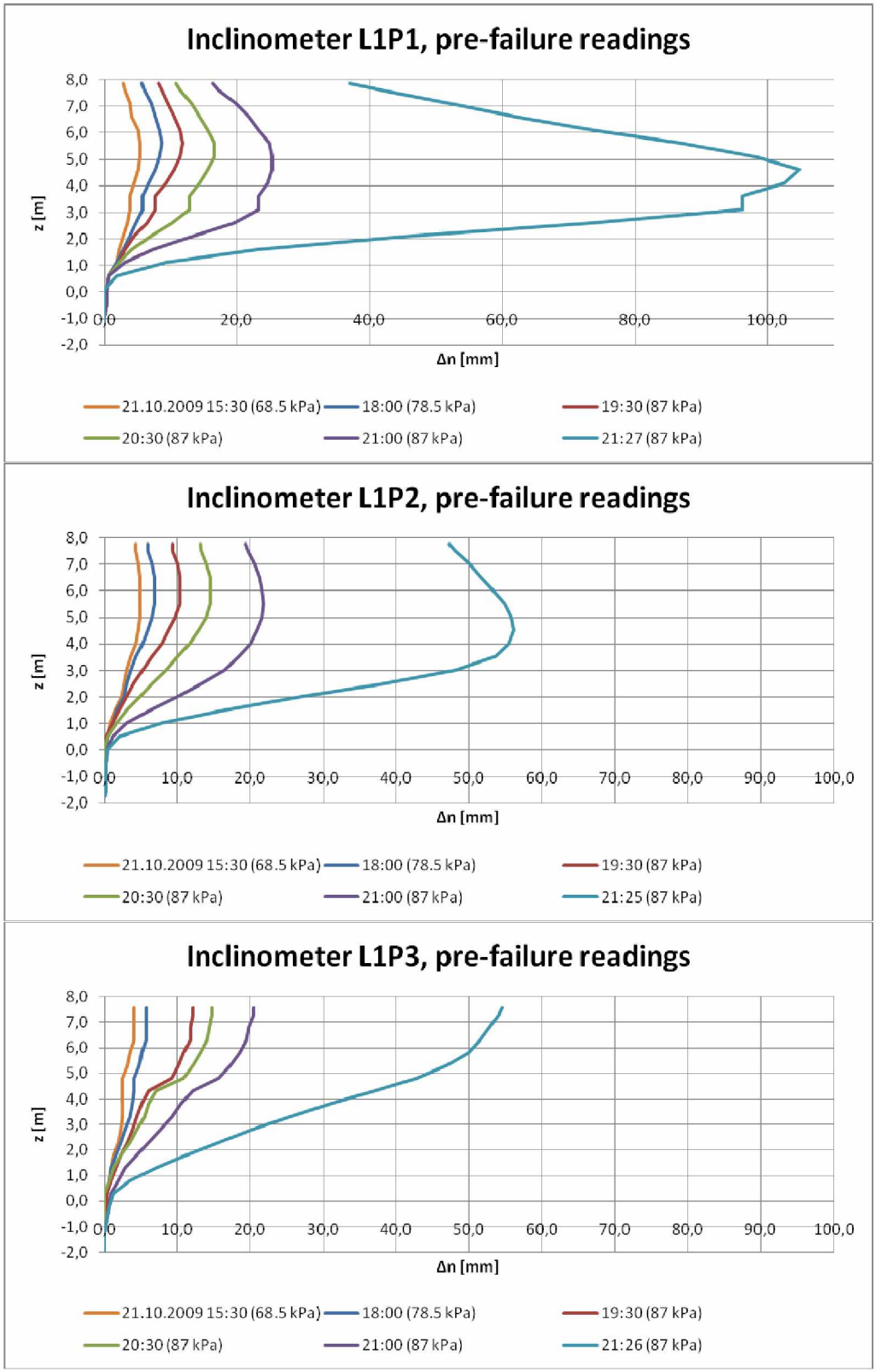

Figure 25 *Inclinometer readings next to cars 1 & 2.*

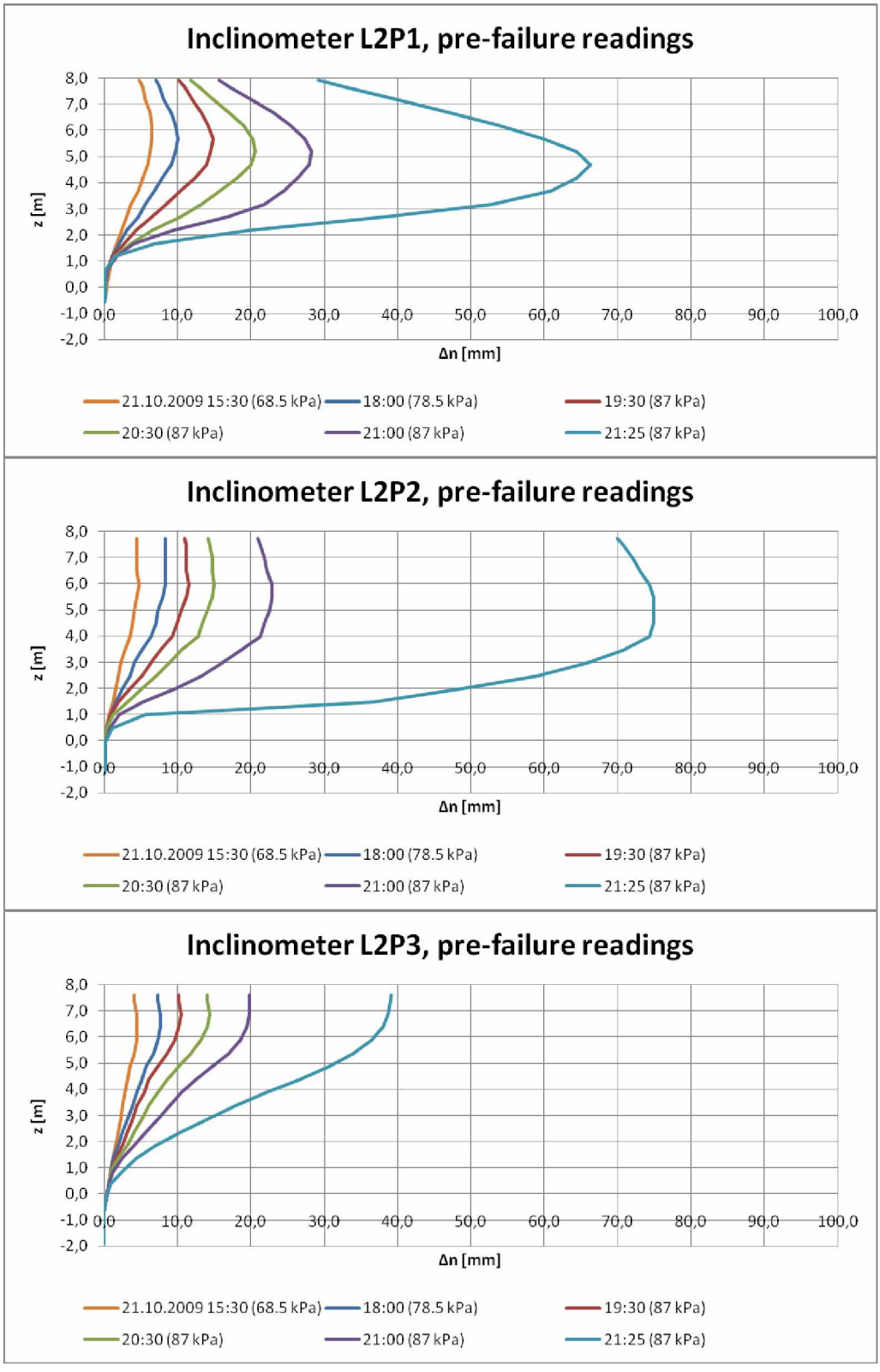

Figure 26 Inclinometer readings next to cars 2 & 3.

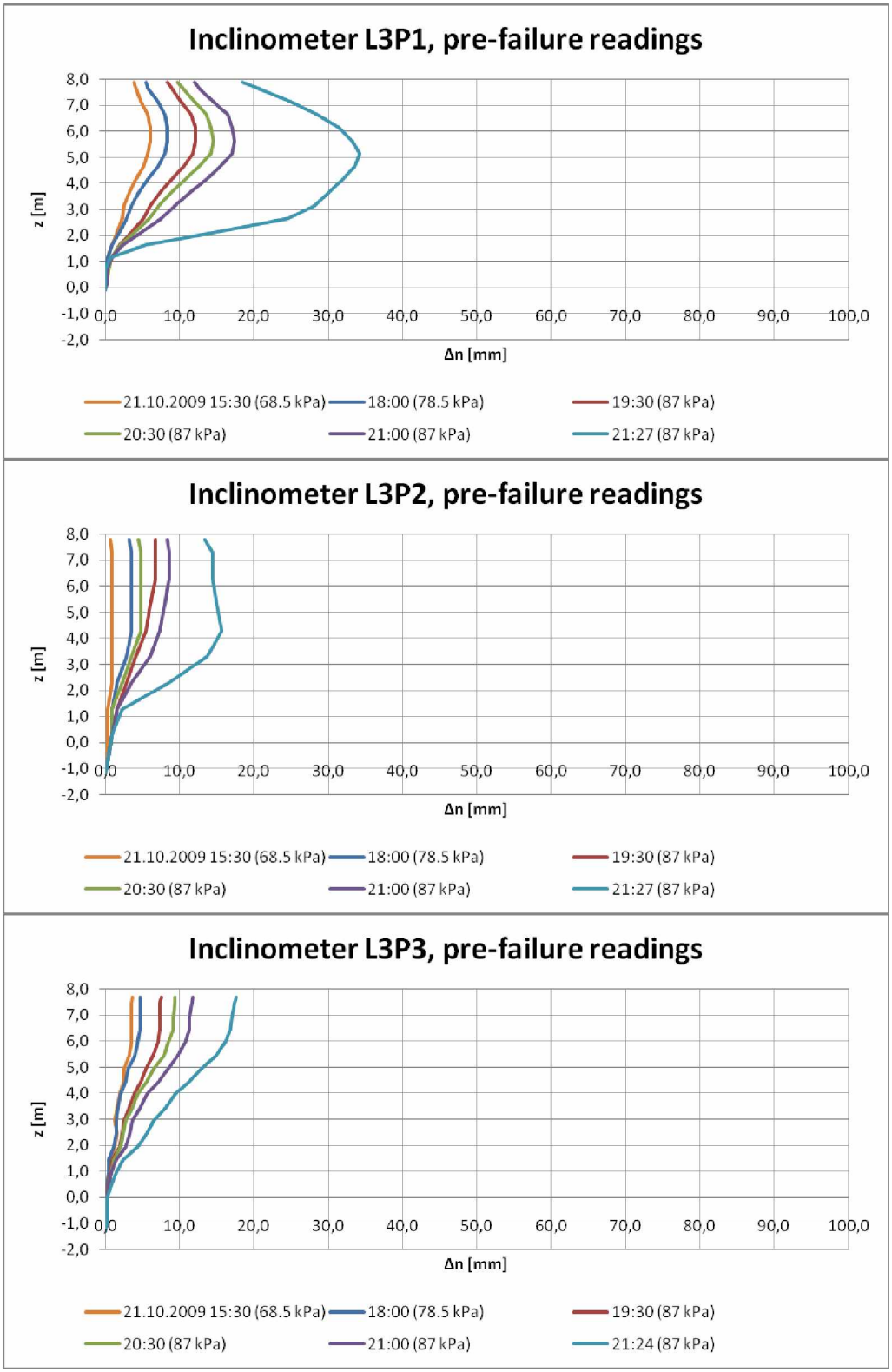

Figure 27 Inclinometer readings next to cars 3 & 4.

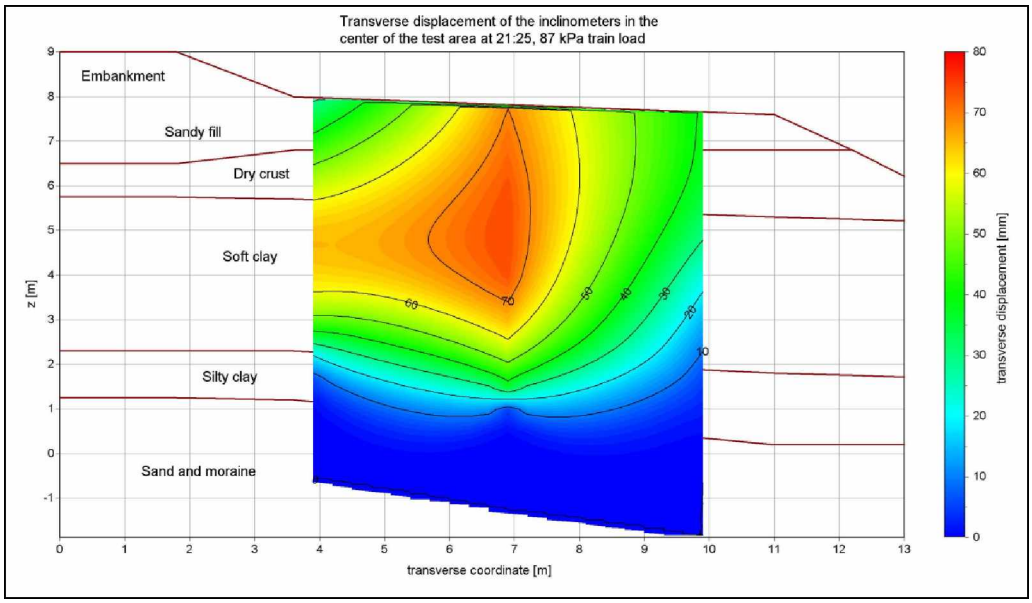

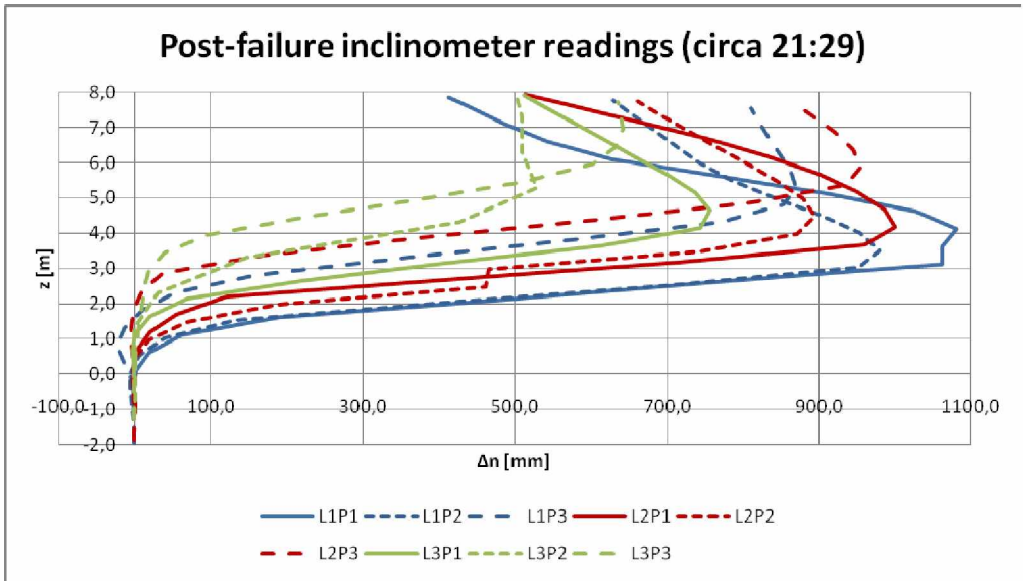

Figure 28 *Post-failure transverse inclinometer readings. Note that these graphs only give a rough sense of the failure geometry. The inaccuracy is due to the inclinometer tubes moving in relation to the soil at failure, and the fact that the most inclined transducers were outside their measuring range.*

5.3 Total stations

Only displacements in the transverse direction are presented here. Longitudinal displacements were negligible and vertical displacements are covered by settlement tube measurements.

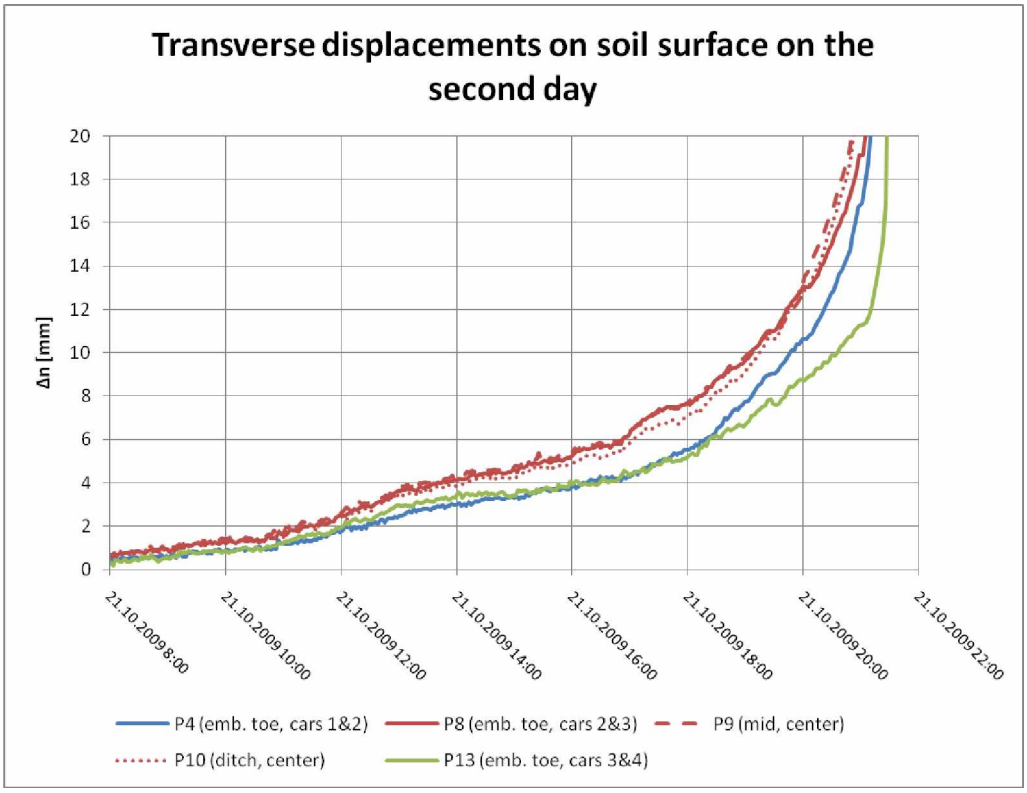

Figure 29 *Selected transverse displacements measured with total stations.*

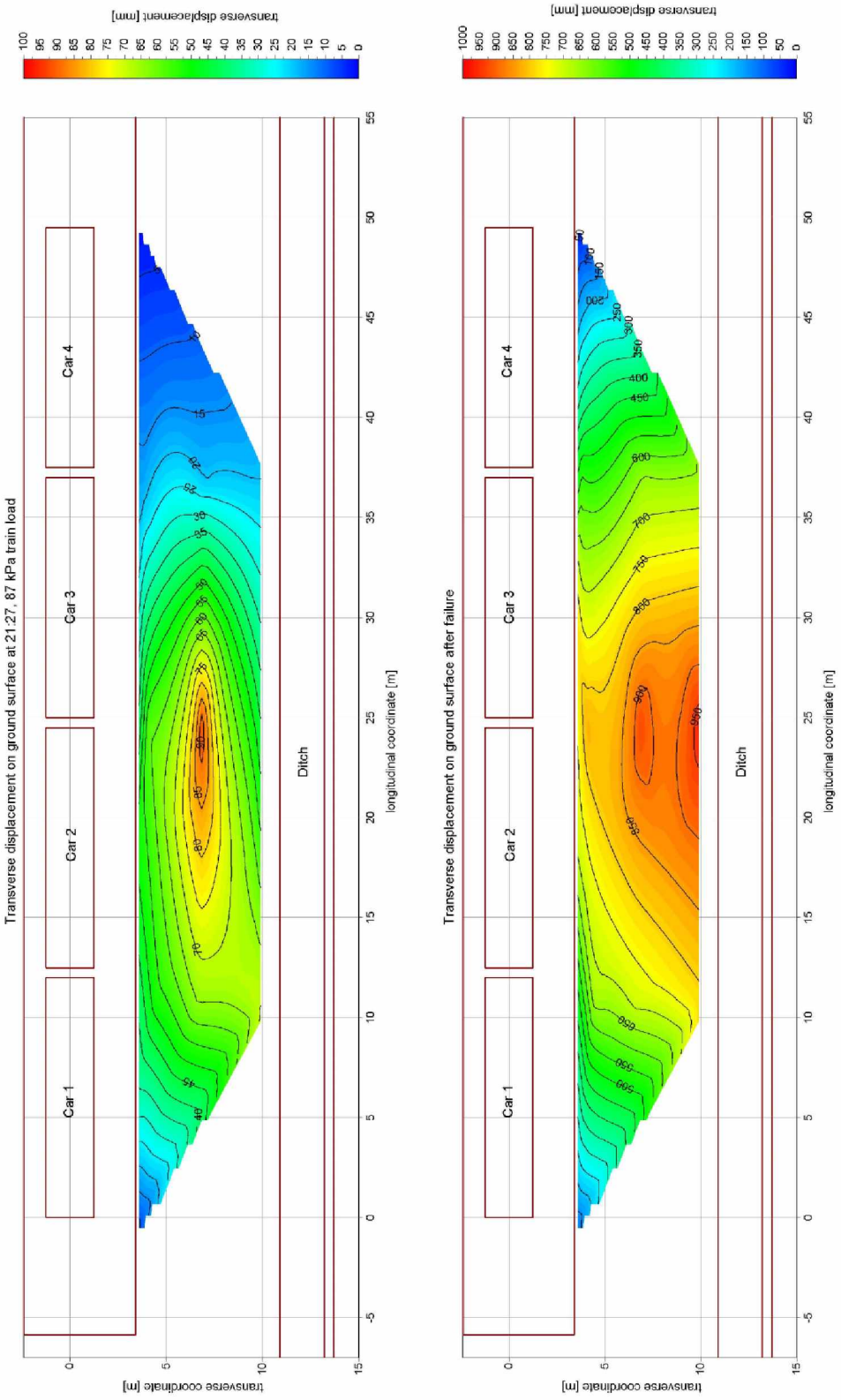

Figure 30 *Transverse displacements right before failure and after the failure, measured with total stations. Note the different scales between the pictures.*

5.4 Settlement tubes

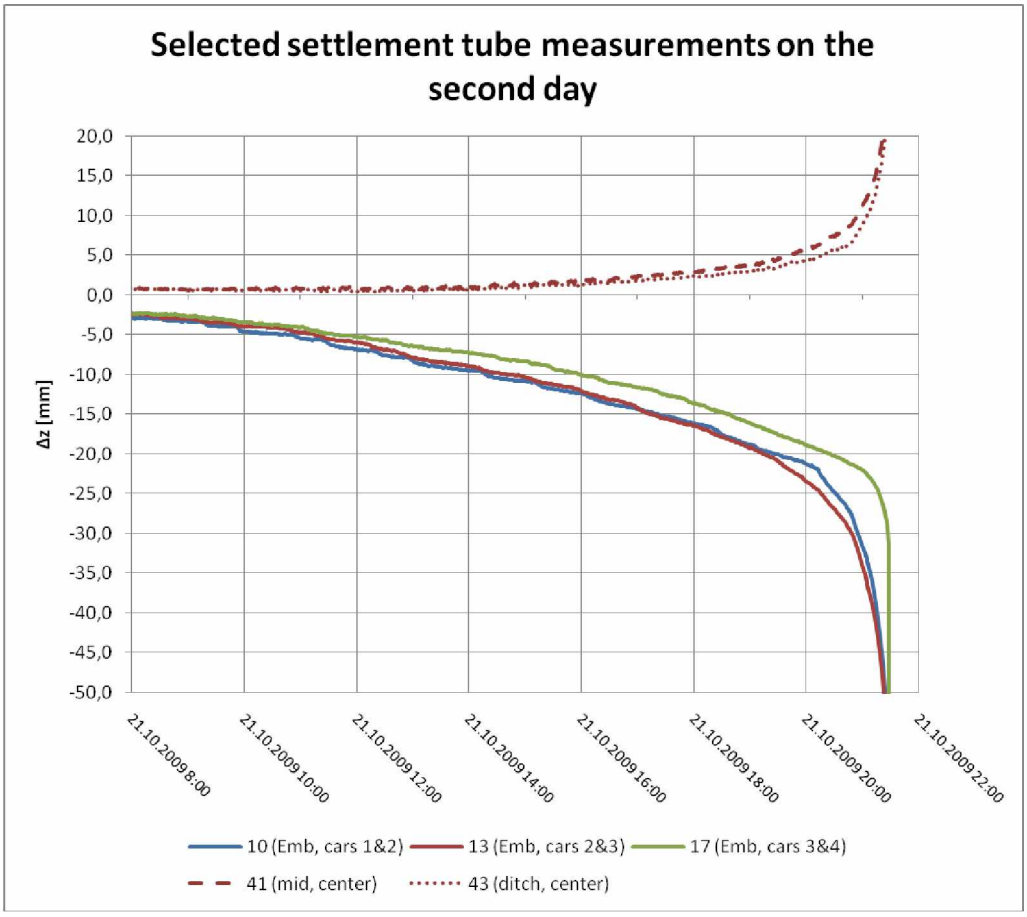

Figure 31 *Selected settlement tube measurements.*

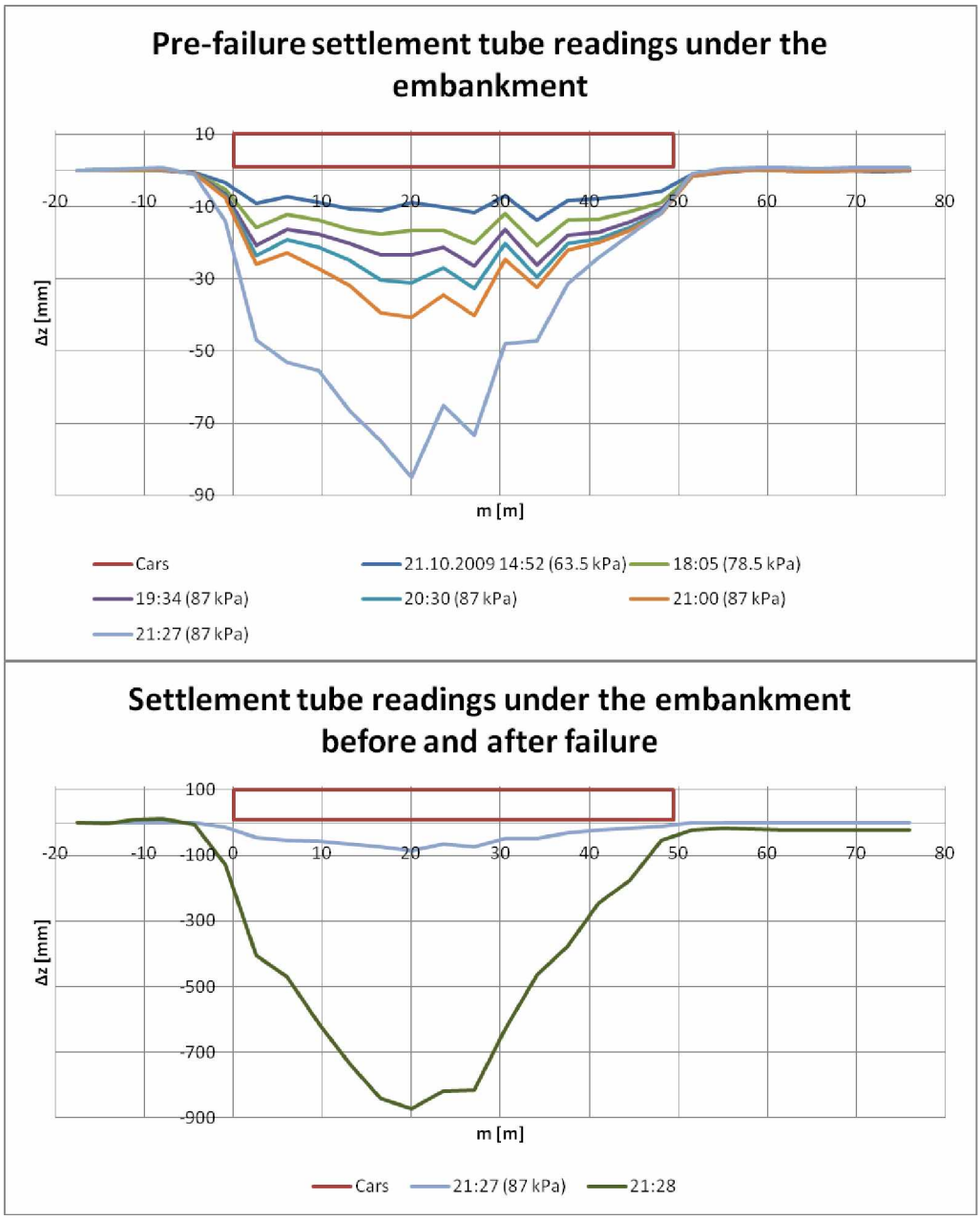

Figure 32 *Settlement tube readings under the embankment.*

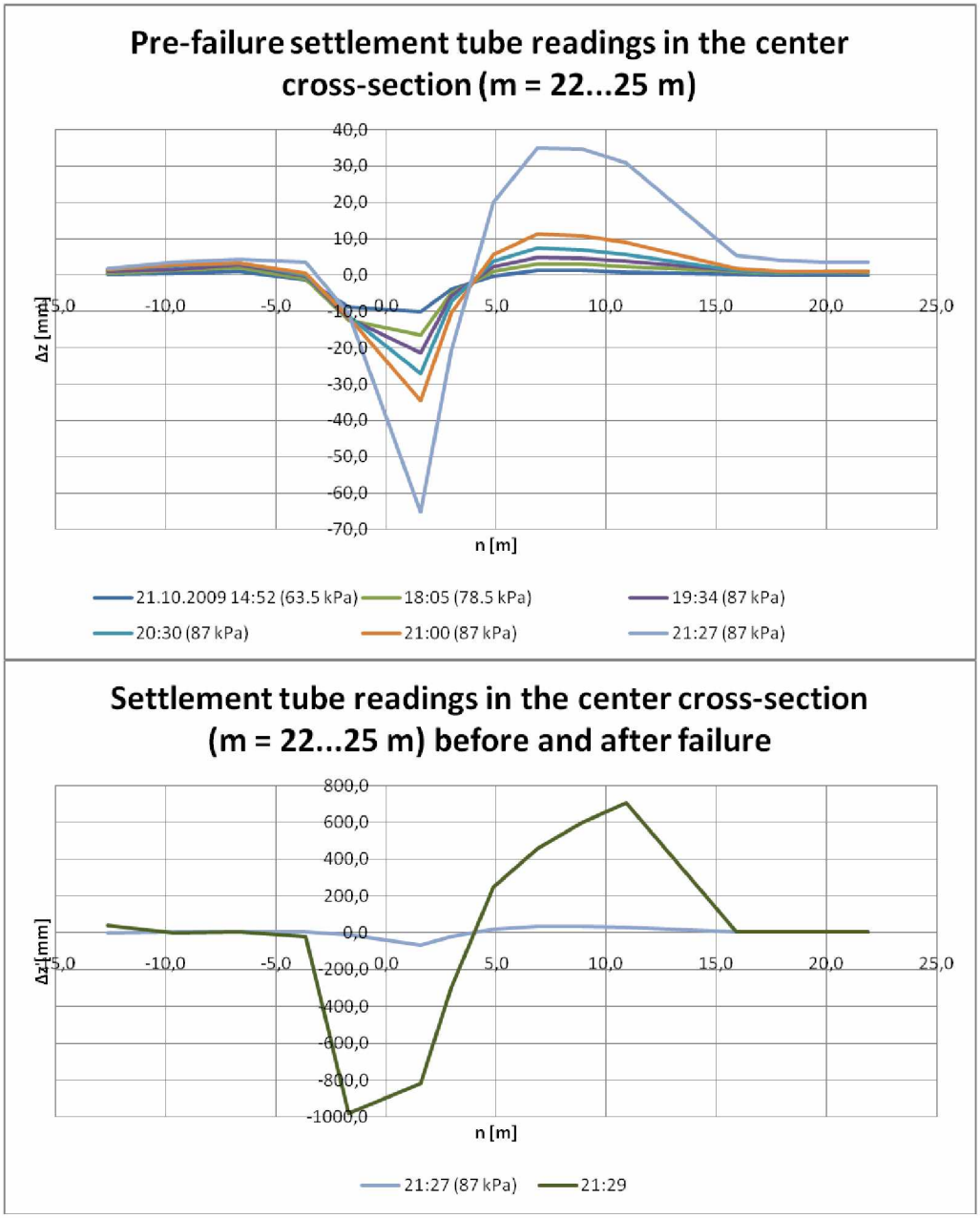

Figure 33 *Settlement tube readings in a cross-section in the middle of the area.*

6 General analysis

6.1 Failure mechanism

The extents of the failure could be best determined from the measuring points of the slip surface tubes (Figure 34). It can be unambiguously postulated that if a measuring point did not move during the experiment, it remained outside the failure zone. Visible cracks on the surface also served as indicators of the extents of the failure, as did the various displacement measurements.

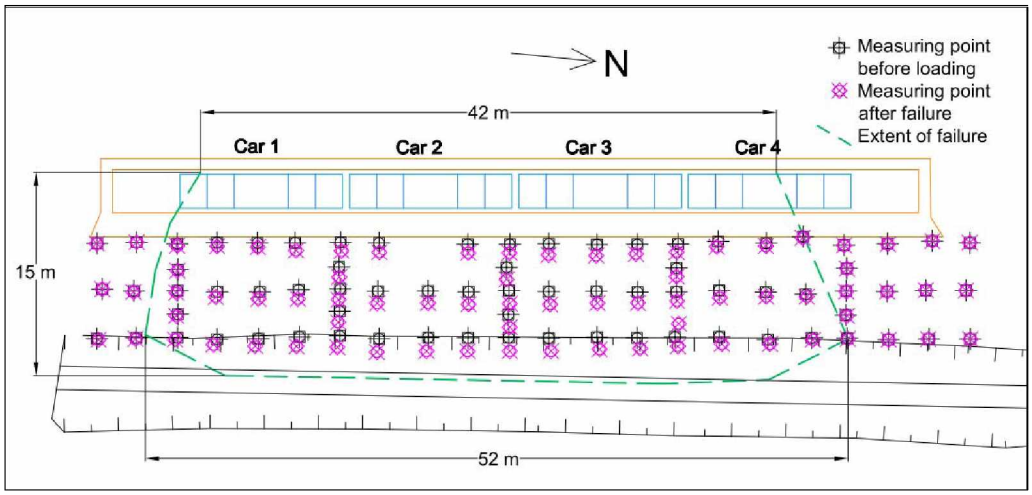

Figure 34 *Extents of the failure approximated from measuring point movements and visual observations.*

Approximating the slip surface shape in a cross-section is not quite as straightforward. The CPTU investigations showed that there were no clear discontinuities in the shear strength of the clay. Instead, the shear strength of the clay seems to have decreased quite uniformly throughout the failed soil mass. This suggests a zone failure instead of a clear slip surface. There was still a certain zone in the soil where shear strains were notably higher than in the surrounding soil, which in itself can be considered a slip surface.

Inclinometers give a general idea of the slip zone. Largest shear strains most likely occur where the inclination of the instrument is the largest. Post-failure readings can, however, be considered fairly inaccurate for the following reasons:

- The most inclined transducers were outside their measuring range, thus showing less displacement than actually took place.
- At failure, the inclinometer tubes moved in relation to the surrounding soil (a result of both axial movement and the tube cutting into the soil). As the anchoring of the bottom end of the tubes most likely fails at failure, the net movement of the inclinometer is very difficult to determine.
- Both aforementioned factors also complicate the calculation of the height reduction needed for the determination of vertical transducer distance at high strains.

For these reasons, the pre-failure inclinometer readings can be considered vastly more accurate for approximating the slip surface location than post-failure readings.

The flexible slip surface tubes were not very useful for approximating the slip surface shape, as the bends that formed at failure were much more gradual than expected. The bend depths were measured with a flexible cable that had a 50 cm long stiff rod at its end. Had the rod been shorter, it would have resulted in deeper readings and vice versa. As depth measurements were made also before the experiment, the tubes that gave the same depth readings before and after were useful in determining the limits of the failure area.

In addition to other measurements, the pore pressure transducers actually provided good information on the slip surface location. During initial loading the excess pore pressure consisted almost entirely of the external load increase. As the clay began to yield, the further increase in excess pore pressure (see next chapter for a more detailed analysis of pore pressure response) was most notable near the slip surface. The placement of pore pressure transducers turned out very successful, as this effect was very clearly visible.

When all available data and observations are combined, the major slip surface shape (or rather, a zone of large shear strains) can be fairly well approximated (Figure 35). The active end started behind the sleepers, from where it descended steeply downwards. The lowest point of the slip surface was under the embankment toe (at ≈+2.5 m height), near the lower boundary of the soft clay area. From there the slip surface curved gradually upwards, ending at the bottom of the ditch. The general shape is very much reminiscent of a Prandtl type bearing capacity failure. This seems logical, as the large external load and fairly low embankment make for a loading situation much like a strip footing.

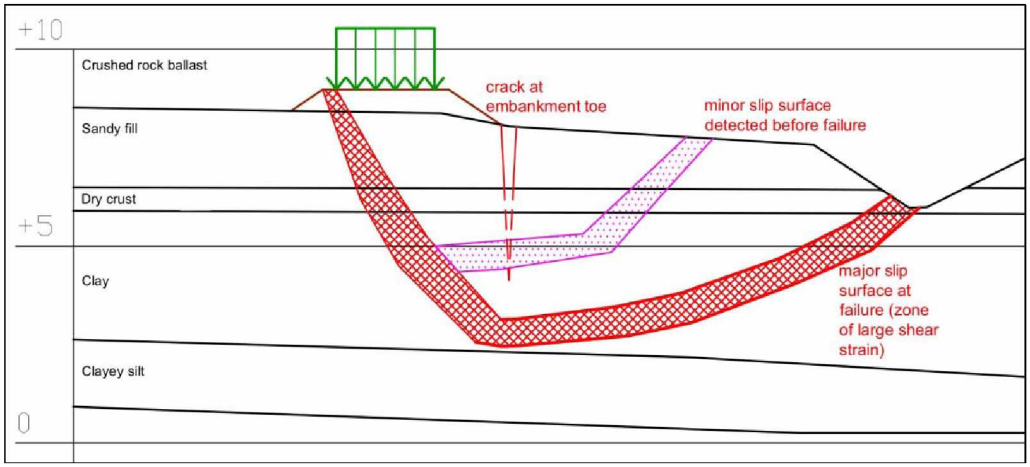

Figure 35 *Estimated slip surface in the middle of the test area.*

During the late stages of loading (beginning at ca. 18:00 on the second day, load at 78 kPa), some pore pressure transducers under the embankment indicated irregularly decreasing pore pressure. This can be considered a true phenomenon (as opposed to equipment malfunction), since many transducers showed generally similar behaviour, but at different times. The hypothesis for the phenomenon was that the transducers were located in the steep active part of the slip zone, where the soil mass on the

"failure side" moved laterally away from the larger immobile soil mass. This caused a drop in total stress, effectively mobilising active earth pressure in that part of the failure zone.

After ca. 19:00 (load ≈83 kPa) some of the pore pressure transducers under the embankment centreline and toe began to indicate accelerating growth of excess pore pressure, as opposed to the near-linear increase during the initial loading. Similar changes in behaviour occurred after 20:30 between the embankment and ditch and slightly later by the ditch. After ca. 21:00 all pore pressure transducers indicated continuously accelerating growth which continued until failure at 21:28.

The very high excess pore pressure under the embankment toe (max. 65 kPa) was most likely a result of the kinematic properties of the failure mechanism. The mechanism can be roughly divided into two parts: the embankment, where large settlements occurred at failure, and parts away from the embankment, where the soil rose. The transition between these opposite-moving parts was brittle, as is evidenced by the fairly wide and deep crack that formed at the embankment toe. In the "corner" of the slip surface large "kinematic" forces and strains were most likely present at failure, thus resulting in large excess pore pressure.

A minor slip surface in the centre part of the eventual failure area was also detected before failure, mostly by transverse displacement measurements (inclinometers and total station measurements). The passive end of the minor slip surface was located somewhere between the edge of the ditch and the level of inclinometer L2P2 and prism P9. The final failure might well have occurred along this smaller surface instead of the eventual larger surface. In pre-experiment stability calculations such a small failure was seen as a distinct possibility, albeit less probable than a failure reaching the bottom of the ditch.

While the final failure area was about 50 m wide, the initial failure began in a significantly smaller area. While the actual failure did take only a few seconds, certain phases could be discerned. The failure first began under car number 2 and part of car 1. Car 3 followed closely, but car 4 that was located on a thinner clay layer than the other cars came down several seconds later than the others. The initial failure width was not at all clearly defined, but a gradual progression from the center parts toward the ends of the embankment can be distinguished.

While the final failure area was about 50 m wide, initial failure began in a significantly smaller area. While the actual failure did take only a few seconds, certain phases could be discerned. The failure began under car number 2 and part of car 1. The initial failure width was thus ca. 20 m, although not at all clearly defined.

6.2 Pore pressure response, rate effects and factor of safety

As clay is loaded in undrained conditions, the normally consolidated region is often considered isotropically elastic. At this point the excess pore pressure buildup corresponds to total mean stress increase (a constant p' stress path). When the clay is sheared further, it begins to yield. In the undrained state the net volumetric strain must be zero. As the clay yields and the initial soil structure begin to break, plastic compression usually occurs. This must be offset by elastic expansion, i.e. a reduction in effective mean stress. This means that further excess pore pressure caused by yielding of the clay is generated in addition to the pore pressure component caused by increase of total mean stress p.

During the initial loading in the experiment the excess pore pressure corresponded roughly to the total mean stress increase in the clay. The soil was still mostly normally consolidated. As the loading was continued, the stress path crossed the initial yield surface, yielding began and soil behaviour became increasingly elasto-viscoplastic. From then on, the pore pressure response became increasingly detached from external load increase. A notable change in soil behavior occurred gradually after external loading exceeded about 75 kPa, as pore pressure and deformation increase began to accelerate progressively from the embankment out. Although the clay had most likely reached its normally consolidated state well before that at least under and close to the embankment, likely the viscose rate effects kept the excess pore pressure from increasing notably before reaching a certain point.

For design and modelling purposes the pore pressure increase is often considered to occur nearly instantaneously when external load is applied. The deformation properties of clay are however highly time-dependent due to undrained creep and correspondingly the pore pressure response is also time-dependent (see e.g. Holzer et al 1973 and Augustesen et al 2004).

Essentially, fast rates of loading on saturated normally consolidated clay would result in less excess pore pressure than with slow rates of loading, and vice versa (Figure 36). A very fast loading that takes the stress state close to failure may at first result in fairly small excess pore pressure. If the load is then kept constant, additional pore pressure will build up with time as per the viscoplastic properties of the clay. This was observed in the late stages of the experiment.

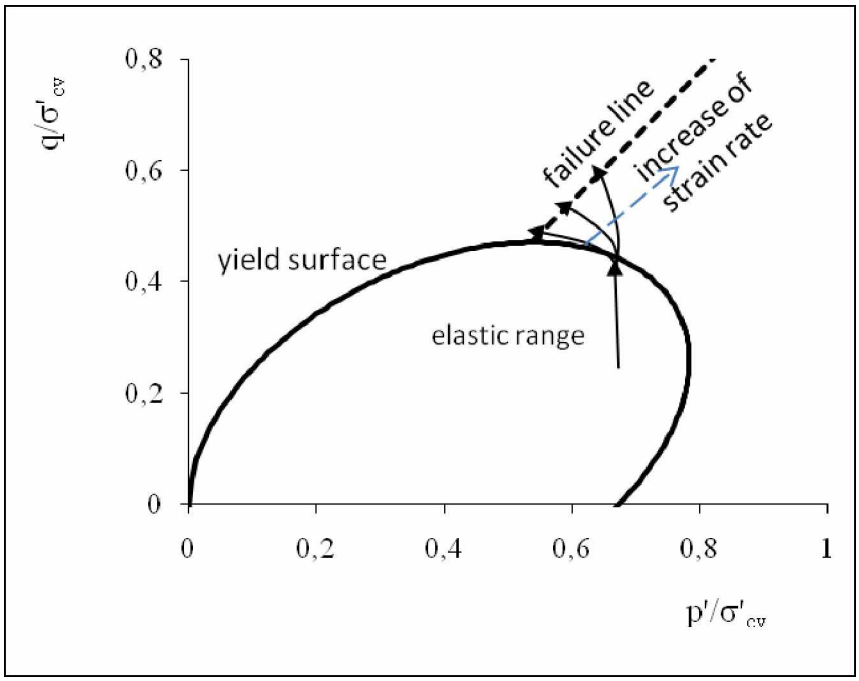

Figure 36 *Effect of loading rate on the effective stress path and shear strength. A conceptual figure. (Lehtonen et al 2011)*

When considering a very quickly applied load on clay, the undrained creep of the clay will cause a time-dependent increase of excess pore pressure from the very initial values right after load application. Effectively, the *factor of safety will decrease* for some time following the construction or other load application. Another conceptual representation in (p', q) space is that effective mean stress p' is reduced as a function of time, thus moving the stress state closer to the failure envelope.

A train coming to a standstill on an embankment built on clay is an extreme example of the effect of undrained creep on stability. For example: A large load is applied instantaneously, and at first the excess pore pressure is fairly small (smaller than would occur if the load was applied at a slower rate). If the large load then remains constant, over time excess pore pressure will increase, moving the effective stress state closer to failure. If the inherent stability of the embankment is not adequate, failure may occur.

Because of the time-dependency of pore pressure response, a clearly defined failure load could not be determined in the embankment failure experiment. Had the final load been smaller than the actualised 87 kPa, the failure would have happened later. The opposite would have been true if a larger load would have been applied. When examining the various measurements, it seems that qualitative changes began to occur at around 80 kPa loading.

Advanced FEM analyses of the experiment have been made using an elasto-viscoplastic soil model (Mansikkamäki et al 2011). The analyses indicate that the ultimate undrained pore pressure state (maximum excess pore pressure, lowest strength) would have been reached if the load would have been applied during a period of over 14 days. According to calculations the corresponding failure load would have been ca. 70 kPa. (Figure 37)

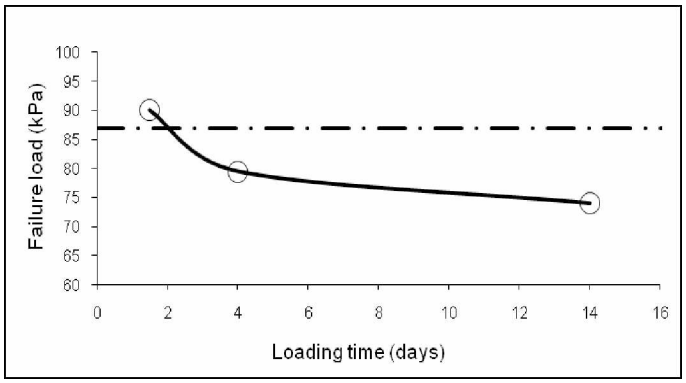

Figure 37 *Effect of loading rate on failure load of the embankment, from FEM analysis with an elasto-viscoplastic soil model. (Mansikkamäki et al 2011)*

While the stability of an embankment will again increase with time due to consolidation and the related dissipation of excess pore pressure, this happens at a much longer time-scale when compared to the viscoplastic pore pressure response governed by undrained creep. It can be postulated that the design value of undrained shear strength should preferably correspond to the strength obtained at the peak pore pressure. This peak pore pressure is most likely reached after undrained creep has continued for some time, but before any significant pore pressure dissipation due to consolidation has occurred.

While there is no need to explicitly take into account the excess pore pressure in $\varphi = 0$ calculations (using s_u), rate effects still apply and are a considerable factor when determining soil strength and failure load of a given design case. In Finnish and Scandinavian engineering practice undrained shear strength is often measured in situ by vane shear testing. The rate of shearing used in the procedure is standardized in Finland as 0.1 °/s. The measured value is usually reduced by an empirically determined factor that is a function of the plastic properties of the clay (usually wL of Ip). The reduction is used to take into account anisotropy and the rate effects (among other factors). The part of the correction related to rate effects is needed because the shearing rate in the standardized test is much larger than what usually is the case in true-life failures. True undrained shear strength is thus lower in the actual failures than what the standard vane shear test will indicate. There is however much uncertainty as to the correct assumptions regarding rate effects, as true rates of loading and shearing are often extremely difficult to predict beforehand.

7 Aspects of stability monitoring

Extensive stability monitoring data was collected before and during the failure. The data also had adequate overlap with different instruments, which made it possible to compare and review the reliability of the various measurements.

A general trend for all measurements could be observed. During the initial loading (until about 78–80 kPa external load, around 18:00–19:00 on the second day of loading), the measured quantities increased fairly linearly or at a slightly accelerating rate. During the second day the loading rate was decreased gradually. As saturated clay is a viscose material, displacements and stress changes in the soil are not only functions of external loading, but also of time and loading rate. A "near-linear" initial response to loads well below failure may still be considered a conceptual aid in interpreting the experiment data.

When the clay was loaded further, it began to yield progressively. Thereafter, all quantities began to increase at an accelerating rate several times higher than during the initial loading (thus the initial response can be considered "linear" despite the slight acceleration exhibited). This qualitative change in behaviour generally occurred first under or near the embankment and then gradually toward the ditch.

From a 'qualitative standpoint', this abrupt change of behaviour, i.e. a change in gradient, was a clear indicator of an impending failure, more so than the absolute measured values themselves. The absolute value of pore pressure is, however, essential information for undrained effective stress stability calculations. For any quantitative plastic stability analysis (e.g. FEM analysis), absolute displacement values are equally important (calibration of calculation parameters, etc).

It must yet be noted that the observed behaviour applies directly only to soft, plastic clay (and in the strictest sense, only to the clay at the experiment site). Different soils have different stress-strain and time-strain properties and as such their pre-failure behaviour differs accordingly.

7.1 Positioning of instruments

Of the measured quantities, the best indicators for an impending failure were embankment settlement (measured by settlement tubes, total stations), excess pore pressure, transverse displacement near the embankment toe (measured by inclinometers, total stations) and ground rise some distance away from the embankment (measured by settlement tubes, total stations).

Measurement of the settlement of the embankment has certain merits when compared to the other displacement quantities. In this experiment, the absolute displacement values were generally larger than other displacement vectors (e.g. transverse displacements or ground rise further away). That makes for easier identification of stability problems as proportionally less data is "lost" in various measurement and interpretation inaccuracies. In addition, monitoring of the embankment itself gives the earliest possible warning. This is due to the fact that the degree of mobilisation at any given time is most likely largest under or near the loaded embankment. A slight progression from the embankment out was evident in

the experiment, as the changes in pore pressure and displacement increase rates were first observed near the embankment. When considering short-term stability in the undrained state ("end of construction"), there is no danger of confusing the occurring settlement with consolidation settlement, as these occur on completely different timescales.

To measure embankment settlement, an instrument must be installed in, on or under the embankment, preferably near the centreline. In general, when measuring vertical displacements, lateral placement of an instrument is vital. In the case of this failure experiment, practically no vertical displacements were measured at the embankment toe. When considering an embankment failure on horizontal surroundings, the soil mass movement due to an embankment failure resembles a seesaw with the active part moving down while the passive part moves up. If an instrument happens to be positioned at the "seesaw pivot point", no vertical movements will be observed. When planning the instrumentation of a given embankment, the most likely failure mechanisms and slip surfaces should be analysed and identified, and the lateral instrument positions determined accordingly.

In some cases vertical displacements can also be measured further away from the embankment, as there will be upward soil displacements within the eventual slip surface near the passive end of the failure mass. It can, however, be considered a fairly difficult task to position the instrument correctly, as the true failure may differ greatly from initial predictions.

Transverse (horizontal) displacements can be observed everywhere within the failure mass, with the possible exception of the embankment centreline. In addition, the large settlements of the embankment may distort the measurement (due to bending of inclinometer tubes, tilting of prisms, etc.). It appears that the best position for measuring transverse displacements is the embankment toe or any other spot close to the embankment that does not exhibit excessive vertical displacements.

The most suitable position for pore pressure measurements is likely where external loading causes a significant total stress increase, i.e. under the embankment or the embankment toe. If there is need to measure the pore pressure caused by the yielding of clay (which would be a good indicator of an impending failure, see Section 6.2), the transducer should be positioned in the eventual failure zone (slip surface). However, being able to measure yield-induced pore pressure with a single transducer requires much luck even if highly advanced analyses are conducted. There were enough instruments in test area, and extensive preplanning was conducted to ensure that several pore pressure transducers were located in the eventual shear zone.

7.2 Suitability and functioning of the instruments

Several types of instruments, many of them suitable for monitoring embankment stability, were used to gather data in the experiment. The instruments most likely usable in real monitoring cases were pore pressure transducers, automatic inclinometers, robotic total stations and settlement tubes.

The choice of an instrument for stability monitoring depends on many factors:

- Quantity to be measured
- Instrument capabilities (accuracy, etc.)
- Level of automated operation (needs and abilities)
- Duration of monitoring
- Long-term serviceability of the instrument
- Environment and surroundings (urban/rural, site accessibility, etc.)
- etc.

Here, only the instruments used in the experiment are considered.

7.2.1 Pore pressure transducers

Pore pressure transducers can be considered a near-necessary complement for displacement measurements. The strain-type pore pressure transducers used in the experiment operated generally well; only a small number of them malfunctioned. Careful de-aeration of the porous stone is required prior to installation to avoid inaccurate readings. Especially when dealing with such a large number of units as in this experiment, extreme care must be taken in applying the individual calibration constants and variables into the system.

While no long-term testing was conducted with the pore pressure transducers, they are most probably fairly well suited for long-term monitoring as they are well shielded from the elements due to their underground location. The most failure-prone items are above-ground systems such as wiring, data loggers and computers. Corroding or short-circuiting solder points might be a problem in some conditions, as well as the clogging of the porous stone in front of the pressure membrane.

7.2.2 Inclinometers

The automatic inclinometers were generally accurate and functioned well. They measured inclination both laterally (transversely) and in the direction of the embankment (longitudinally).

The transverse inclinometer readings were clear and consistent with other measurements, but there were some problems with the longitudinal readings due to slightly inaccurate installation. Longitudinal displacements were much smaller than transverse displacements (the direction of the total displacement vector is nearly perpendicular to the embankment). If the unit is installed slightly off its correct direction so that the axes of measurement do not coincide with the desired geometry, the reading in the direction of the smaller component will be greatly erroneous. The effect of a slightly off-direction installation is close to negligible in the transverse direction.

7.2.3 Total stations

As total stations allow very accurate measurement of displacements in any direction, they can be considered highly useful in monitoring the stability of various structures. Modern robotic total stations coupled with monitoring and data acquisition software can be used for completely automatic long-term monitoring.

In this experiment there were, however, problems with the total stations themselves moving. Although periodic corrections of the instrument locations were made using fixed prisms on nearby buildings, the data was slightly inaccurate (the data presented in this paper has been corrected and smoothed for instrument movement). Unfortunately the total stations could not be positioned further away due to line-of-sight constraints.

Another issue against using automatic total stations for long-term monitoring is the requirement for a clear line of sight from the instrument to the prisms. In the case of a railway embankment, there may be problems with vegetation in summer. In winter the prisms may be covered in snow or damaged by ice flying from passing trains. The measurements may also be impeded if the prism face gets covered by water droplets.

7.2.4 Settlement tubes

The new automatic settlement tubes showed great promise for accurate long-term monitoring of vertical displacements. They functioned reliably and gave accurate results. In addition, they can be very cost-effective considering the relative simplicity of the design and the ability to automatically monitor even tens of points along a length of several hundred metres. Thus far slightly over 100 m long tubes have been used. The limit for the length of the tube would likely be determined by the difficulty of handling a very long tube.

The settlement tubes also seem to work well in long-term monitoring. They have been field-tested in frost heave monitoring from 2009 onwards on a railway track section in southern Finland (Luomala 2010). The measurements have been accurate, consistent and reliable.

Problems may occur if the settlement tube is subjected to sudden temperature changes. That may for example cause the fluid in the tube to flow from one part to another, resulting in inaccurate pressure readings. That can be averted by installing the tube deep enough in the soil, so that temperature in the tube will not change rapidly. The measurements may also be sensitive to dynamic loads that might cause pressure waves in the fluid.

8 Conclusions and notes on further research

A comprehensively instrumented full-scale railway embankment failure experiment was carried out in 2009. The embankment was built on clay subsoil and brought to failure with an external load that simulated a stopping train. A large amount of data on the loading stage and failure was collected. Certain instruments suitable for monitoring the stability of embankments were tested and evaluated.

The time-dependency of pore pressure and displacement response due to the high rate of loading was made evident by the experiment. During most of the loading, the displacements and excess pore pressure grew at a moderate, nearly linear rate. Near the end of loading, the clay began to yield progressively, and displacements and pore pressure began to increase at a continuously accelerating rate. Failure occurred two hours after loading was ended. The gradients of displacement and pore pressure change were largest right before the failure.

It seems apparent that due to the clearly time-dependent pore pressure response, a clearly defined failure load cannot be determined for fast undrained loading on clay, but instead the failure load depends on soil properties, rate of loading and time elapsed. The same can be said of the transient factor of safety for a given load and time.

For practical design purposes, the factor of safety should still be calculated according to the maximum pore pressure/minimum shear strength for a given load (theoretically reached after enough time has passed after load application, but before any significant consolidation begins).

For a very quickly loaded embankment (e.g. a railway embankment with a train coming to a standstill) on clay the factor of safety will likely decrease for some time until the maximum pore pressure is reached in the undrained state. This time-dependency is a matter to be taken into account when considering the monitoring of embankments of low stability, as the initial moderate excess pore pressure and displacements might give a false sense of security.

The best indicators of an impending railway embankment failure were found to be accelerating embankment settlement, transverse soil displacements, excess pore pressure response and upward movement of the soil on the sides of the embankment. That is generally in line with previous research (e.g. Hunter & Fell 2003). The choice of monitored quantities and the placement of instruments should be based on case-specific analyses of the probable failure mechanism.

The RASTAPA project (jointly conducted between Tampere University of Technology and the Finnish Transport Agency), of which the embankment failure experiment was a part, will continue at least until 2013. Post-experiment research consists of analysing and further developing advanced stability calculation methods especially for railway embankments, as well as determining the most suitable and cost-effective methods for improving the stability of existing embankments.

In the field of FEM modelling, highly advanced models for soft soils are evaluated (Mansikkamäki et al 2011). The emphasis is on viscoplastic analyses using soil models that account for undrained creep, such as EVP-SCLAY1S and AniCreep. These

models can also account for factors such as anisotropy and destructuration. The initial results seem promising, as these models can be used to accurately model the behavior of clay in undrained conditions.

The downside of highly advanced FEM soil models is that they require a large number of soil parameters that do not always have a direct physical meaning that would enable them to be determined easily from laboratory testing. As such the new advanced models are not yet suitable for everyday design purposes.

In addition to the FEM analyses, two new ways of approximating excess pore pressure in effective stress LEM calculations are being developed (Länsivaara et al 2011). The new methods are meant to be easy to use in normal design calculations. In essence, the two methods assume a yield surface based on the strength parameters of the soil. The yield surface is used to assume an undrained stress path, from which the excess pore pressure is calculated. A new development in pore pressure calculations is to assume failure pore pressure even for factors of safety above 1. This will result in a more accurate representation of the factor of safety that is compatible with total stress stability analyses.

References

Augustesen, A., Liingaard, M., Lade, P. 2004: Evaluation of Time-Dependent Behavior of Soils. International Journal of Geomechanics, 4 (2004), pp. 137-156. American Society of Civil Engineers ASCE.

Holzer, T. L., Höeg, K., Arulanandan, K. 1973: Excess pore pressures during undrained clay creep. Canadian Geotechnical Journal, Vol. 10, No. 1, Feb. 1973, pp. 12–24. National Research Council of Canada.

Hunter, G., Fell, R. 2003: Prediction of impending failure of embankments on soft ground. Canadian Geotechnical Journal, Vol. 40, No. 1, Feb. 2003, pp. 209–220. National Research Council of Canada.

Laaksonen, A. 2005: Liikuntasaumattoman sillan ja maan yhteistoiminta. Master's Thesis. Earth and Foundation Structures, Research report 62. 157 pages., 83 app. pages. Tampere University of Technology, Tampere.

Lehtonen, V. 2010: Ratapenkereen sorrutuskokeen instrumentointi ja analysointi. Liikenneviraston tutkimuksia ja selvityksiä 25/2010. 150 p., 3 app. Finnish Transport Agency, Helsinki.

Lehtonen, V., Länsivaara, T., Luomala, H., Mansikkamäki, J. 2011: A Full-scale railway embankment failure experiment – arrangements and observations. GEORAIL 2011 International symposium, pp. 271–280. IFSTTAR, Paris

Leroueil, S., Magnan, J-P., Tavenas, F. 1990: Embankments on soft clays. Ellis Horwood Series in Civil Engineering. 360 p. Ellis Horwood Ltd, Great Britain.

Leroueil, S., Tavenas, F., Mieussens, C. Peignaud, M. 1978: Construction pore pressures in clay foundations under embankments. Part II: generalized behaviour. Canadian Geotechnical Journal, Vol. 15, No. 1, Feb. 1978, pp. 66–82. National Research Council of Canada.

Luomala, H. 2010: Ratapenkereiden monitorointi. Liikenneviraston tutkimuksia ja selvityksiä 22/2010. 85 p., 2 app. Finnish Transport Agency, Helsinki.

Länsivaara, T., Lehtonen, V., Mansikkamäki, J. 2011: Failure induced pore pressure, experimental results and analysis. 2011 Pan-Am CGS Geotechnical Conference.

Mansikkamäki, J., Lehtonen, V., Länsivaara, T. 2011: Advanced stability analysis of a failure test on an old railway embankment. GEORAIL 2011 International symposium, pp. 291–300, IFSTTAR, Paris

Liikennevirasto

Finnish Transport Agency

ISSN-L 1798-6656
ISSN 1798-6664
ISBN 978-952-255-685-1
www.fta.fi